PHYSICAL REVIEW C **81**, 064310 (2010)

Many-body approach for quartet condensation in strong coupling

Takaaki Sogo and Gerd Röpke
Institut für Physik, Universität Rostock, D-18051 Rostock, Germany

Peter Schuck
Institut de Physique Nucléaire, CNRS, UMR 8608, Orsay F-91406, France Université Paris-Sud, Orsay F-91505, France
Laboratoire de Physique et Modélisation des Milieux Condensés, CNRS, and Université Joseph Fourier, 25 Avenue des Martyrs, Boîte Postale 166, F-38042 Grenoble Cedex 9, France and
Groupe de Physique Theorique Institut de Physique Nucleaire, F-91406 Orsay Cedex, France
(Received 2 April 2010; published 16 June 2010)

The theory for condensation of higher fermionic clusters is developed. Fully self-consistent nonlinear equations for the quartet order parameter in strongly coupled fermionic systems are established and solved. The breakdown of the quasiparticle picture is pointed out. Derivation of numerically tractable approximation is described. The momentum projected factorization ansatz for the order parameter is employed. As a definite example, the condensation of α particles in nuclear matter is worked out.

DOI: 10.1103/PhysRevC.81.064310 PACS number(s): 21.65.−f, 21.60.−n, 67.85.Lm, 74.20.Fg

I. INTRODUCTION

Quartet condensation is relevant in several domains of physics. So far, it has been considered mostly in nuclear physics with the strongly bound α-particle cluster playing a dominant role in certain states of lighter nuclei [1] and, eventually, also in the surface of heavy nuclei, as may be indicated by the observed α-decay processes. α-Particle condensation may eventually occur in compact stars [2]. However, trapping of multicomponent fermionic atoms makes fast progress. The case of trions is already quite advanced, experimentally [3,4] and also theoretically [5–13]. One may be able to trap fermions with four different "colors" in the near future. This is a prerequisite for quartet formation and quartet condensation. Theoretical work on this subject already has appeared [14–18]. The condensation of biexcitons in semiconductors also may be of relevance [19,20].

In the recent past, we published several papers on α-particle condensation in infinite nuclear matter. For instance, we studied the onset of α-particle condensation and evaluated the corresponding critical temperature [21,22] with a procedure analogous to the pairing case via a four-body generalization of the famous Thouless criterion [23]. However, quartet condensation not only is formally much more complicated than condensation of (Cooper) pairs, but also it turns out that also certain aspects of the physics are quite different. The most striking feature is that quartets exist only in the so-called Bose-Einstein condensate (BEC) limit where they do not overlap very much in space. Contrary to the pairing case, quartets cannot strongly intermingle in real space, and therefore, a coherence length much longer than the inter-α-particle distance cannot exist. We give the reason for this different behavior in the main text.

In this article, we treat quartet condensation at zero Kelvin temperature and establish and solve a full nonlinear equation for the quartet order parameter, which is the analog to the gap equation for pairing. A direct solution of such a highly nonlinear four-body problem seems hopeless, even in homogeneous matter. However, we recently showed that a simplifying approximation works very well, at least in the domain of negative chemical potentials, that is, in the strong coupling regime. This approximation consists in making a mean-field ansatz (i.e., a Slater determinant) for the quartet but projected onto zero total momentum as it is relevant for condensation [21]. Such a mean-field treatment may work each time the quartet is in its lowest energy configuration. However, one may think of generalizations for excited configurations as well. Since the four fermions of the quartet are all different in the nuclear case (proton/neutron, spin up/down), all are in the same $0S$ mean-field wave function, and the problem boils down in the end to solving the equation by iterating on this single one-particle mean-field wave function. The same happens, of course, if the four fermions are components of an $F = 3/2$ spin as in [16]. The problem still is complicated but can be solved with effective interactions of separable form. It was shown that that approximation gives results comparable to the four-body Faddeev-Yakubovsky equation with a more realistic interaction in the nuclear case. So, in the present work, we calculate the order parameter equation with the projected mean-field ansatz and a separable potential.

The article is organized as follows: in the next section, we discuss the BCS gap equation. In Sec. III, we show the full expression of the single-particle mass operator for quartet condensation. Because this is too difficult to calculate numerically, we suggest an approximate mass operator in Sec. IV. Before we show the numerical result employed by the approximated mass operator, we discuss in Sec. V the significant difference between pairing condensation and quartet condensation through the different level densities involved in the condensation processes. In Sec. VI, we present the results. Finally, we conclude in the last section. In the appendices, we describe the detailed derivation of the equations and discuss various methods to formulate the order parameter equation for quartet condensation.

II. RECAPITULATION OF THE PAIRING CASE

To prepare the terrain for our procedure in the quartetting case, in this section we rederive standard BCS theory in a way somewhat different than the usual.

The one-body Green's function (GF) for BCS is represented by [24]

$$G_{1;1'}(\omega) = \frac{\delta_{11'}}{\omega - \varepsilon_1 - M^{\rm BCS}_{1;1}(\omega)}, \tag{1}$$

where $M^{\rm BCS}_{1;1}(\omega)$ is the BCS mass operator

$$M^{\rm BCS}_{1;1'}(\omega) = \sum_2 \frac{\Delta_{12}\Delta^*_{1'2}}{\omega + \varepsilon_2}, \tag{2}$$

where

$$\Delta_{12} = -\frac{1}{2}\sum_{34} \bar{v}_{12,34}\langle c_4 c_3\rangle, \tag{3}$$

with $\langle cc\rangle$ being the thermal average of the pair operator.

The indices 1, 2, 3, ... correspond to momentum and spin. In nuclear matter, we have to add isospin. The term $\bar{v}_{12,34}$ is the antisymmetrized matrix element of the two-body interaction ($\bar{v}_{12,34} = -\bar{v}_{12,43} = -\bar{v}_{21,34}$). The single-particle energies ε_i are in principle given by the kinetic energies plus the mean-field shifts. The direct term is in homogeneous matter a constant that can be incorporated into the chemical potential, and the Fock-term gives rise to an effective mass. Because we mostly deal with very-low-density nuclear matter, we do not consider a mass renormalization here. Therefore, in Eq. (1) we have $\varepsilon_1 = k_1^2/(2m) - \mu_1$ with the chemical potential μ_1, which in principle contains the direct part of the mean field. We have attached an index on the chemical potential, since in principle it can depend on the various fermionic components involved. However, in this work, we always consider fully symmetric situations, and henceforth we suppose that the chemical potentials of all fermionic species are equal and therefore drop the index.

Figure 1 is the graphical representation of the BCS mass operator. As shown in Eq. (2) and Figure 1, the BCS mass operator consists of the two-particle–one-hole (2p1h) GF between two-body vertices factorized into two order parameters and the free 1h GF.

On the other hand, the in-medium Schrödinger equation for the order parameter is of the following form:

$$\langle c_2 c_1\rangle = -\frac{1-\rho_1-\rho_2}{\varepsilon_1+\varepsilon_2}\sum_{1'2'}\frac{1}{2}\bar{v}_{12,1'2'}\langle c_{2'}c_{1'}\rangle, \tag{4}$$

where ρ_1 is the occupation number derived from

$$\rho_1 = -\int \frac{d\omega}{2\pi} 2{\rm Im}G_{1;1}(\omega + i\eta) f(\omega), \tag{5}$$

with the Fermi distribution function $f(\omega) = [e^{\omega/T} + 1]^{-1}$ and a positive infinitesimal of η, as indicated.

In the standard BCS theory, pairs in time-reversed states are considered, for example, in Eqs. (3) and (4), by taking $2 = \bar{1}$, $\rho_1 = \rho_{\bar{1}}$, and $\varepsilon_1 = \varepsilon_{\bar{1}}$, where $\bar{1}$ is the time-reversal conjugate of quantum numbers 1. For Eq. (1), we obtain the imaginary part of the one-body Green function as

$$-{\rm Im}G_{1;1}(\omega + i\eta) = \frac{1}{2}\left(1 + \frac{\varepsilon_1}{E_1}\right)\pi\delta(\omega - E_1) + \frac{1}{2}\left(1 - \frac{\varepsilon_1}{E_1}\right)\pi\delta(\omega + E_1) \tag{6}$$

with $\Delta_{1\bar{1}} = \Delta_1$ and $E_1 = \sqrt{\varepsilon_1^2 + \Delta_1^2}$. This is equivalent to solving the usual gap equation at finite temperature, as can easily be deduced from the spectral function obtained from (1) [25,26]:

$$\Delta_1 = -\sum_{1'}\frac{1}{2}\bar{v}_{1\bar{1},1'\bar{1}'}\frac{\Delta_{1'}}{2E_{1'}}\tanh\left(\frac{E_{1'}}{2T}\right). \tag{7}$$

Note that Eq. (4) resembles a particle-particle RPA equation [24] with renormalized occupation numbers. One could therefore also consider Eq. (4) as a single-pole approximation to the so-called renormalized RPA, well known in the literature (see, e.g., Ref. [27]).

III. SINGLE-PARTICLE MASS OPERATOR AND QUARTET CONDENSATION

Formally, it is straightforward to generalize the pairing case to the quartet case. A typical diagram of the mass operator needed for quartet condensation is shown in Fig. 2. As seen, to make the quartet order parameter appear in the single-particle mass operator, we need to express it by the 4p3h GF. To get to it, we must successively open phase space from one particle to 2p1h, to 3p2h, to 4p3h. This needs three interaction vertices on each side, as shown in Fig. 2. Details of the derivation are given in the Appendix B. For the 1p mass operator with quartet condensation, we obtain

$$M^{\rm quartet}_{1;1'}(\omega) = \Gamma^{(4)}_{1234;5678}(\omega)\langle c_8 c_7 c_6 c_5\rangle\frac{\bar{f}_2\bar{f}_3\bar{f}_4 + f_2 f_3 f_4}{\omega + \varepsilon_{234}} \times P_{234;2'3'4'}\langle c^\dagger_{5'}c^\dagger_{6'}c^\dagger_{7'}c^\dagger_{8'}\rangle\Gamma^{(4)*}_{1'2'3'4';5'6'7'8'}(\omega), \tag{8}$$

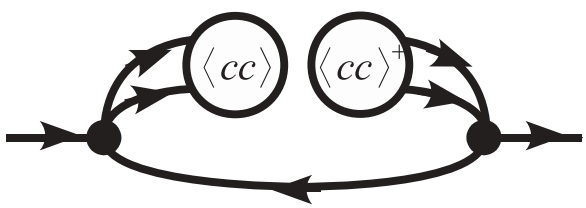

FIG. 1. Graphic representation of the BCS mass operator in Eq. (2).

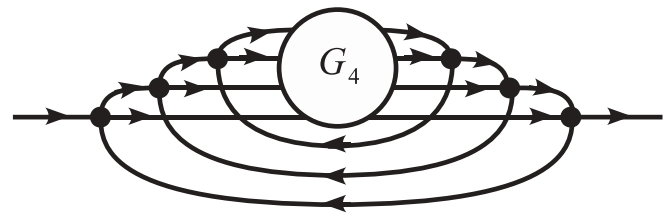

FIG. 2. Diagram for the mass operator.

where summation convention over repeated indices is understood, and

$$P_{123;1'2'3'} = \begin{vmatrix} \delta_{11'} & \delta_{12'} & \delta_{13'} \\ \delta_{21'} & \delta_{22'} & \delta_{23'} \\ \delta_{31'} & \delta_{32'} & \delta_{33'} \end{vmatrix}. \tag{9}$$

The effective four-body vertex $\Gamma^{(4)}$, evaluated perturbatively to the third order in the interaction, is

$$\begin{aligned} \Gamma^{(4)}_{1234;5678}(\omega) = \Gamma^{(3)}_{12'3';4'5'6'}(\omega) \frac{1}{\omega - \varepsilon_{4'5'6'} + \varepsilon_{2'3'}} \\ \times \left[\frac{1}{2} \bar{v}_{4'4,58} \delta_{2'2} \delta_{3'3} \delta_{5'6} \delta_{6'7} + \frac{1}{2} \bar{v}_{5'4,68} \delta_{2'2} \delta_{3'3} \right. \\ \times \delta_{4'5} \delta_{6'7} + \frac{1}{2} \bar{v}_{6'4,78} \delta_{2'2} \delta_{3'3} \delta_{4'5} \delta_{5'6} - \frac{1}{2} \bar{v}_{2'8,24} \\ \left. \times \delta_{3'3} \delta_{4'5} \delta_{5'6} \delta_{6'7} - \frac{1}{2} \bar{v}_{3'8,34} \delta_{2'2} \delta_{4'5} \delta_{5'6} \delta_{6'7} \right], \end{aligned} \tag{10}$$

$$\begin{aligned} \Gamma^{(3)}_{123;456}(\omega) = \frac{1}{2} \bar{v}_{12',3'4'} \frac{1}{\omega - \varepsilon_{3'4'} + \varepsilon_{2'}} \left[\frac{1}{2} \bar{v}_{3'2,45} \delta_{2'3} \delta_{4'6} \right. \\ \left. + \frac{1}{2} \bar{v}_{4'3,45} \delta_{2'2} \delta_{3'6} - \frac{1}{2} \bar{v}_{2'6,23} \delta_{3'4} \delta_{4'5} \right], \end{aligned} \tag{11}$$

where $\varepsilon_{123\ldots} = \varepsilon_1 + \varepsilon_2 + \varepsilon_3 + \cdots$ and $\bar{f}_i = 1 - f_i$ with the Fermi distribution function $f_i = f(\varepsilon_i)$.

One may wonder why in (10) and (11) no Fermi function factors appear with the propagators. However, this is a general feature of vertices coupling lower configuration spaces to higher ones. A famous example in the literature is given by coupling 1p1h and 2p2h spaces as this appears in the damping of zero-sound modes (see, e.g., [28]). One may notice that the absence of Pauli blocking factors opens up phase space and therefore enhances the coupling.

One can ask the question whether in Eq. (8) the uncorrelated mean-field 3h GF should be used. One may think to include the hole GFs into the self-consistent cycle or even include higher correlations. However, one should notice that in BCS this is not done and that in Eq. (2) the mean-field 1h GF is used. This has a good reason, because BCS theory is based on a variational wave function, which fully respects the Pauli principle. Should a self-consistent hole GF be used in (2), this property would be lost. We, therefore, also stick to the mean-field hole GFs in the quartet case.

We also need the in-medium four-body Schrödinger equation for the order parameter, in analogy with the pairing case shown in Eq. (4) in the previous section. It is given by

$$\varepsilon_{1234} \langle c_4 c_3 c_2 c_1 \rangle + \sum_{1'2'3'4'} V_{1234;1'2'3'4'} \langle c_{4'} c_{3'} c_{2'} c_{1'} \rangle = 0, \tag{12}$$

where

$$\begin{aligned} V_{1234;1'2'3'4'} = (1 - \rho_1 - \rho_2) \tfrac{1}{2} \bar{v}_{12;1'2'} \delta_{33'} \delta_{44'} + (1 - \rho_1 - \rho_3) \\ \times \tfrac{1}{2} \bar{v}_{13;1'3'} \delta_{22'} \delta_{44'} + \text{permutations}. \end{aligned} \tag{13}$$

Details are given in [22] and Appendix C.

We consider symmetric (nuclear) matter. In this case, we can give a fully symmetric order parameter of exchange between two particles with respect to momenta:

$$\langle c_4 c_3 c_2 c_1 \rangle \to \phi_{\vec{k}_1, \vec{k}_2, \vec{k}_3, \vec{k}_4} \chi_0, \tag{14}$$

where the spin-isospin singlet wave function is represented by χ_0, and we consider here a spin-isospin independent two-body interaction:

$$\bar{v}_{12,34} \to v_{\vec{k}_1 \vec{k}_2, \vec{k}_3 \vec{k}_4} \left(\delta_{s_1 s_3} \delta_{t_1 t_3} \delta_{s_2 s_4} \delta_{t_2 t_4} - \delta_{s_1 s_4} \delta_{t_1 t_4} \delta_{s_2 s_3} \delta_{t_2 t_3} \right), \tag{15}$$

with s_i (t_i) of spin (isospin) index. Here, $v_{\vec{k}_1 \vec{k}_2, \vec{k}_3 \vec{k}_4}$ is symmetric with respect to the exchange of the momenta: $v_{\vec{k}_1 \vec{k}_2, \vec{k}_3 \vec{k}_4} = v_{\vec{k}_2 \vec{k}_1, \vec{k}_3 \vec{k}_4} = v_{\vec{k}_1 \vec{k}_2, \vec{k}_4 \vec{k}_3}$.

Then, Eq. (12) is explicitly written as

$$\begin{aligned} \sum_{i=1}^{4} \varepsilon_i \phi_{\vec{k}_1 \vec{k}_2 \vec{k}_3 \vec{k}_4} + \int \prod_{i=1}^{4} \frac{d^3 k_i'}{(2\pi)^3} \times \big[(1 - \rho(\vec{k}_1) \\ - \rho(\vec{k}_2)) v_{\vec{k}_1 \vec{k}_2, \vec{k}_1' \vec{k}_2'} (2\pi)^3 \delta(\vec{k}_3 - \vec{k}_3') (2\pi)^3 \delta(\vec{k}_4 - \vec{k}_4') \\ + (1 - \rho(\vec{k}_1) - \rho(\vec{k}_3)) v_{\vec{k}_1 \vec{k}_3, \vec{k}_1' \vec{k}_3'} (2\pi)^3 \delta(\vec{k}_2 - \vec{k}_2') \\ \times (2\pi)^3 \delta(\vec{k}_4 - \vec{k}_4') + \text{permutations} \big] \phi_{\vec{k}_1' \vec{k}_2' \vec{k}_3' \vec{k}_4'} = 0. \end{aligned} \tag{16}$$

A sketch of the quartet mass operator is shown in Fig. 3.

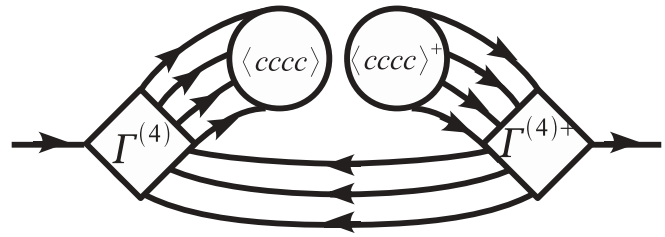

FIG. 3. Graphic representation of the mass operator for α condensation in Eq. (8).

IV. APPROXIMATE QUARTET MASS OPERATOR

From Eqs. (10) and (11) it becomes evident that the full evaluation of the 1p $\leftrightarrow$ 4p3h vertices are too complicated to be evaluated exactly. However, with quite reasonable approximations, one arrives at a numerically manageable expression. Because this discussion involves lengthy, quite technical details, we relegate it to Appendix D and only give the final result here:

$$M^{\text{quartet}}_{1;1}(\omega) = \sum_{234} \frac{\tilde{\Delta}_{1234} (\bar{f}_2 \bar{f}_3 \bar{f}_4 + f_2 f_3 f_4) \tilde{\Delta}^*_{1234}}{\omega + \varepsilon_{234}}, \tag{17}$$

where the quartet gap matrix $\tilde{\Delta}_{1234}$ is given by

$$\tilde{\Delta}_{1234} = \lambda' \tfrac{1}{2} \bar{v}_{12,1'2'} \delta_{33'} \delta_{44'} \langle c_{1'} c_{2'} c_{3'} c_{4'} \rangle. \tag{18}$$

The graphical representation of the approximate M^{quartet} is shown in Fig. 4.

In Eq. (18), we put a renormalization factor λ' in front of the vertex, which effectively accounts for the approximations considered; see Appendix D. However, it is very fortunate that the final result is independent of the value of λ', and therefore one also may drop it. This somewhat surprising effect is due to self-consistency and self-readjustment of the solution. It is demonstrated in Appendix E for the simple case of ordinary pairing.

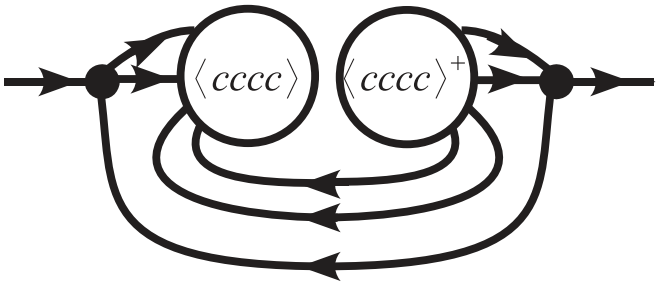

FIG. 4. Graphical representation of the approximate α-BEC mass operator $M^{\rm quartet}$ of Eq. (17).

The complexity of the calculation still is further much reduced for the order parameter (14) with our mean-field ansatz projected on zero total momentum, as already very successfully employed in [21]:

$$\phi_{\vec{k}_1\vec{k}_2,\vec{k}_3\vec{k}_4} = \varphi(|\vec{k}_1|)\varphi(|\vec{k}_2|)\varphi(|\vec{k}_3|)\varphi(|\vec{k}_4|) \times (2\pi)^3\delta(\vec{k}_1+\vec{k}_2+\vec{k}_3+\vec{k}_4). \tag{19}$$

It should be pointed out that this product ansatz with four identical $0S$ single-particle wave functions is typical for a ground-state configuration of the quartet. Excited configurations with wave functions of higher nodal structures may eventually be envisaged for other physical situations. We also mention that the momentum-conserving δ function induces strong correlations among the four particles and therefore is a nontrivial variational wave function.

For the two-body interaction of $v_{\vec{k}_1\vec{k}_2,\vec{k}_3\vec{k}_4}$ in Eq. (15), we employ the same separable form as done already in our previous publication on the quartet critical temperature in Ref. [21]:

$$v_{\vec{k}_1\vec{k}_2,\vec{k}_3\vec{k}_4} = \lambda w\left(\frac{\vec{k}_1-\vec{k}_2}{2}\right) w\left(\frac{\vec{k}_3-\vec{k}_4}{2}\right) \times (2\pi)^3\delta(\vec{k}_1+\vec{k}_2-\vec{k}_3-\vec{k}_4), \tag{20}$$

with the form factor $w(\vec{k}) = w(|\vec{k}|) = e^{-k^2/b^2}$. An example for strength and range parameters is given in Sec. VI.

With these simplifications, the mass operator (17) is independent of spin and isospin, and therefore it can be reduced to the following four-fold integral:

$$M^{\rm quartet}(k_1,\omega) = \frac{1}{(4\pi^2)^4}\int_0^\infty dK K^2 \int_{-1}^1 dt_1 \int_0^\infty dk k^2 \int_{-1}^1 dt \frac{\bar f(|\vec K-\vec k_1|)\bar f\left(\left|\frac{\vec K}{2}+\vec k\right|\right)\bar f\left(\left|\frac{\vec K}{2}-\vec k\right|\right) + f(|\vec K-\vec k_1|)f\left(\left|\frac{\vec K}{2}+\vec k\right|\right)f\left(\left|\frac{\vec K}{2}-\vec k\right|\right)}{\omega+\varepsilon_{\vec K-\vec k_1}+\varepsilon_{\frac{\vec K}{2}+\vec k}+\varepsilon_{\frac{\vec K}{2}+\vec k}} \times \left[w\left(\left|\vec k_1-\frac{\vec K}{2}\right|\right)\right]^2\left[\varphi\left(\left|\frac{\vec K}{2}+\vec k f\right|\right)\right]^2\left[\varphi\left(\left|\frac{\vec K}{2}-\vec k\right|\right)\right]^2\left[\int_0^\infty dk'k'^2\int_{-1}^1 dt' w(k')\varphi\left(\left|\frac{\vec K}{2}+\vec k'\right|\right)\varphi\left(\left|\frac{\vec K}{2}-\vec k'\right|\right)\right]^2, \tag{21}$$

with $t_1 = (\vec K\cdot\vec k_1)/(Kk_1)$, $t = (\vec K\cdot\vec k)/(Kk)$, and $t' = (\vec K\cdot\vec k')/(Kk')$. Here, we represented the Fermi distribution function as $f_1 \to f(k_1) = f(\varepsilon_1)$. In this expression, any strength factor of the vertices has been dropped; see our previous argument and Appendix E. For the imaginary part of this expression, an energy-conserving δ function comes instead of the full denominator, and then the four-dimensional (4D) integral can be reduced to a three-dimensional (3D) one. How this goes in detail is again explained in Appendix F. The real part of $M^{\rm quartet}$ is then obtained from the imaginary part via a dispersion integral:

$$\mathrm{Re}M^{\rm quartet}(k,\omega+i\eta) = -\mathcal{P}\int_{-\infty}^\infty \frac{d\omega'}{\pi}\frac{\mathrm{Im}M^{\rm quartet}(k,\omega'+i\eta)}{\omega-\omega'}, \tag{22}$$

where $\mathcal{P}$ denotes the Cauchy principal value.

The occupation numbers are finally obtained from

$$\rho(k) = -\int\frac{d\omega}{2\pi}2\mathrm{Im}G(k,\omega+i\eta)f(\omega) = \int\frac{d\omega}{2\pi}\frac{-2\mathrm{Im}M^{\rm quartet}(k,\omega+i\eta)}{[\omega-\varepsilon(\vec k)-\mathrm{Re}M^{\rm quartet}(k,\omega+i\eta)]^2+[\mathrm{Im}M^{\rm quartet}(k,\omega+i\eta)]^2}f(\omega). \tag{23}$$

The equation for the order parameter (19) is formally not changed from Eqs. (4)–(7) of [21], but the occupation numbers are calculated self-consistently with the equation. For completeness, we again give the equations for the single-particle wave function $\varphi(k)$

$$\mathcal{A}(k)\varphi(k) + 3\mathcal{B}(k) + 3\mathcal{C}(k)\varphi(k) = 0, \tag{24}$$

where

$$\begin{aligned}
&\mathcal{A}(k)\\
&= \int \frac{d^3k_2}{(2\pi)^3}\frac{d^3k_3}{(2\pi)^3}\frac{d^3k_4}{(2\pi)^3}\left(\frac{k^2}{2m}+\frac{k_2^2}{2m}+\frac{k_3^2}{2m}+\frac{k_4^2}{2m}-4\mu\right)\\
&\quad\times\varphi^2(k_2)\varphi^2(k_3)\varphi^2(k_4)(2\pi)^3\delta(\vec{k}+\vec{k}_2+\vec{k}_3+\vec{k}_4)\\
&= \frac{1}{(2\pi)^4}\int dK\,K^2\int_{-1}^{1}dt\left(\frac{k^2}{2m}+\frac{3}{2m}P^2-4\mu\right)\\
&\quad\times\varphi^2(P)\int dk'k'^2\int_{-1}^{1}dt'\varphi^2(k')\varphi^2(P'),
\end{aligned}\tag{25}$$

$$\begin{aligned}
&\mathcal{B}(k)\\
&= \int \frac{d^3k_2}{(2\pi)^3}\frac{d^3k_3}{(2\pi)^3}\frac{d^3k_4}{(2\pi)^3}\frac{d^3k_1'}{(2\pi)^3}\frac{d^3k_2'}{(2\pi)^3}\\
&\quad\times[1-\rho(k)-\rho(k_2)]\lambda w\left(\frac{\vec{k}-\vec{k}_2}{2}\right)\\
&\quad\times w\left(\frac{\vec{k}_1'-\vec{k}_2'}{2}\right)(2\pi)^3\delta(\vec{k}+\vec{k}_2-\vec{k}_1'-\vec{k}_2')\varphi(k_1')\varphi(k_2)\\
&\quad\times\varphi(k_2')\varphi^2(k_3)\varphi^2(k_4)(2\pi)^3\delta(\vec{k}+\vec{k}_2+\vec{k}_3+\vec{k}_4)\\
&= \frac{\lambda}{(2\pi)^6}\int dK\,K^2\int_{-1}^{1}dt[1-\rho(k)-\rho(P)]w(Q)\varphi(P)\\
&\quad\times\int dk'k'^2\int_{-1}^{1}dt'w(Q')\varphi(k')\varphi(P')\\
&\quad\times\int dk''k''^2\int_{-1}^{1}dt''\varphi^2(k'')\varphi^2(P''),
\end{aligned}\tag{26}$$

$$\begin{aligned}
&\mathcal{C}(k)\\
&= \int \frac{d^3k_2}{(2\pi)^3}\frac{d^3k_3}{(2\pi)^3}\frac{d^3k_4}{(2\pi)^3}\frac{d^3k_2'}{(2\pi)^3}\frac{d^3k_3'}{(2\pi)^3}[1-\rho(k_2)-\rho(k_3)]\\
&\quad\times\lambda w\left(\frac{\vec{k}_2-\vec{k}_3}{2}\right)w\left(\frac{\vec{k}_2'-\vec{k}_3'}{2}\right)(2\pi)^3\delta(\vec{k}_2+\vec{k}_3-\vec{k}_2'-\vec{k}_3')\\
&\quad\times\varphi(k_2)\varphi(k_2')\varphi(k_3)\varphi(k_3')\varphi^2(k_4)(2\pi)^3\delta(\vec{k}+\vec{k}_2+\vec{k}_3+\vec{k}_4)\\
&= \frac{\lambda}{(2\pi)^6}\int dK\,K^2\int_{-1}^{1}dt\varphi^2(P)\int dk'k'^2\\
&\quad\times\int_{-1}^{1}dt'[1-\rho(k')-\rho(P')]w(Q')\varphi(k')\varphi(P')\\
&\quad\times\int dk''k''^2\int_{-1}^{1}dt''w(Q'')\varphi(k'')\varphi(P'').
\end{aligned}\tag{27}$$

with

$$\begin{aligned}
P &= \sqrt{K^2+k^2+2Kkt},\\
P' &= \sqrt{K^2+k'^2+2Kk't'},\\
P'' &= \sqrt{K^2+k''^2+2Kk''t''},\\
Q &= \sqrt{K^2/4+k^2+Kkt},\\
Q' &= \sqrt{K^2/4+k'^2+Kk't'},\\
Q'' &= \sqrt{K^2/4+k''^2+Kk''t''}.
\end{aligned}$$

As mentioned, in these equations the occupation numbers $\rho(k)$ are calculated self-consistently from Eq. (23).

Because of its particular importance, before the presentation of the results, we first discuss in the following section the 3h level density.

V. THREE-HOLE LEVEL DENSITY

In what follows, a crucial role is played by the 3h propagator entering the mass operator. Because its influence on quartet condensation is radically different from the corresponding 1h propagator in the pairing case, we pay special attention to it in

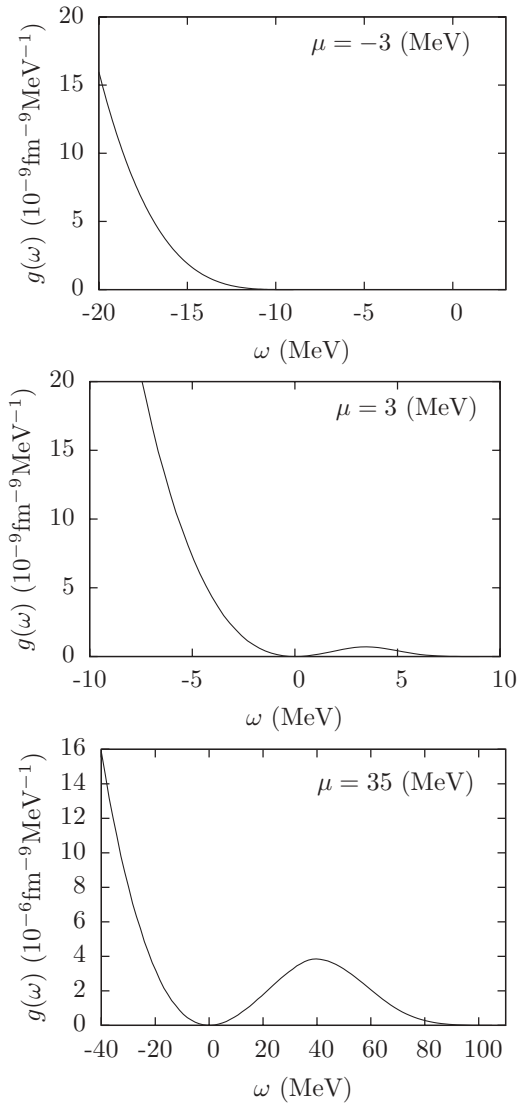

FIG. 5. The 3h level densities defined in Eq. (29) for various values of the chemical potential μ at zero temperature.

this section. In mean-field approximation, we write

$$\frac{(\bar{f}_1\bar{f}_2\bar{f}_3 + f_1f_2f_3)}{\omega + \varepsilon_{123}} = G^{(3h)}(k_1, k_2, k_3; \omega), \tag{28}$$

where in the right-hand side we dropped spin and isospin indices because we consider unpolarized (nuclear) matter. We immediately see a strong difference with the pairing case. There, only a single-hole line enters whose numerator is (see previous section) $\bar{f}_1 + f_1 = 1$; see Eq. (2). Therefore, no single-particle occupation numbers appear in the numerator of a single-hole propagator. This difference between the 3h and 1h propagators leads to strong consequences. This is best demonstrated in Fig. 5 with the 3h level density

$$\begin{aligned} g(\omega) &= -\int \frac{d^3k_1}{(2\pi)^3}\frac{d^3k_2}{(2\pi)^3}\frac{d^3k_3}{(2\pi)^3}\mathrm{Im}G^{(3h)}(k_1, k_2, k_3; \omega + i\eta) \\ &= \int \frac{d^3k_1}{(2\pi)^3}\frac{d^3k_2}{(2\pi)^3}\frac{d^3k_3}{(2\pi)^3}(\bar{f}_1\bar{f}_2\bar{f}_3 + f_1f_2f_3) \\ &\quad \times \pi\delta(\omega + \varepsilon_1 + \varepsilon_2 + \varepsilon_3) \\ &= \frac{m}{(2\pi)^5}\int_0^{k_{\max}} dkk^2 \int_0^{K_{\max}} dK K^2 p \\ &\quad \times [\bar{f}(k)\bar{F}(K, p) + f(k)F(K, p)], \end{aligned} \tag{29}$$

where

$$k_{\max} = \sqrt{2m(3\mu - \omega)}, \tag{30}$$

$$K_{\max} = \sqrt{4m(3\mu - \omega) - 2k^2}, \tag{31}$$

$$p = \sqrt{3m\mu - m\omega - \frac{k^2}{2} - \frac{K^2}{4}}, \tag{32}$$

and

$$F(K, p) = \int_{-1}^{1} dt f\left(\left|\frac{\vec{K}}{2} + \vec{p}\right|\right) f\left(\left|\frac{\vec{K}}{2} - \vec{p}\right|\right), \tag{33}$$

$$\bar{F}(K, p) = \int_{-1}^{1} dt \bar{f}\left(\left|\frac{\vec{K}}{2} + \vec{p}\right|\right) \bar{f}\left(\left|\frac{\vec{K}}{2} - \vec{p}\right|\right), \tag{34}$$

with $t = \vec{K}\cdot\vec{p}/(Kp)$.

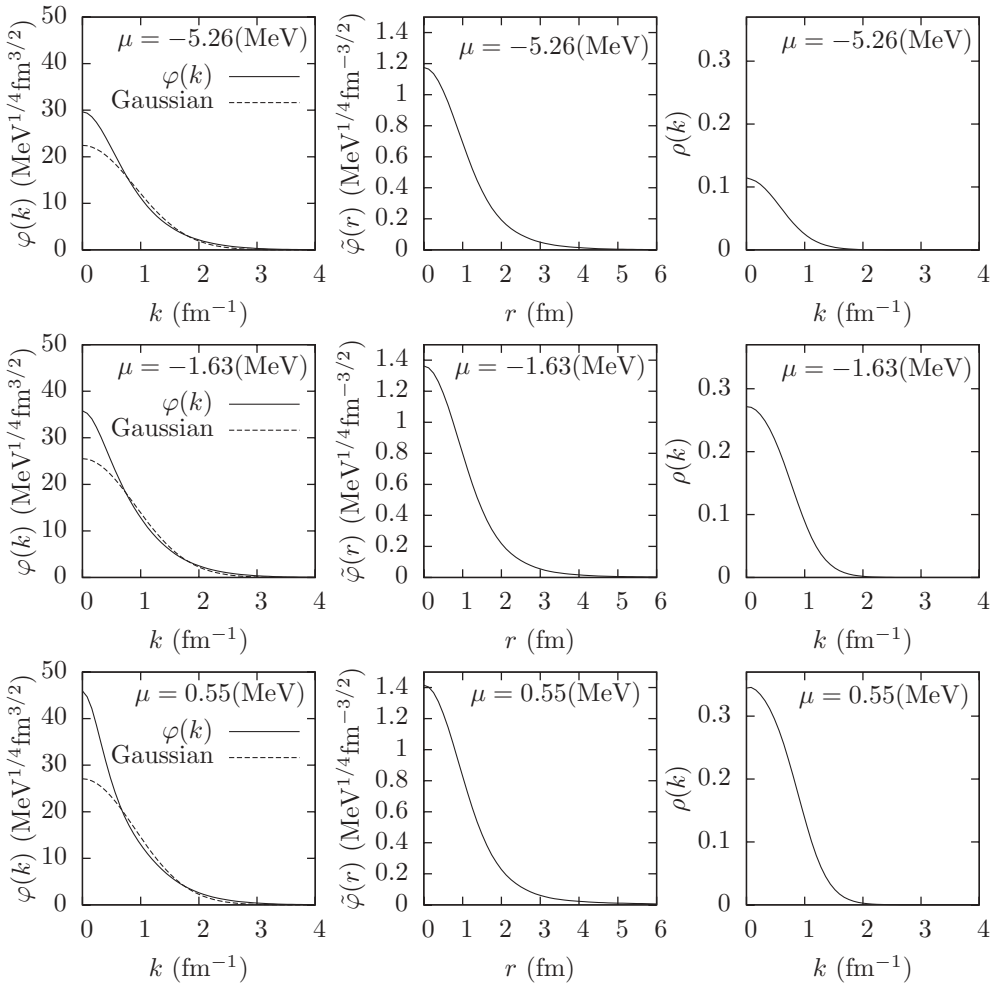

FIG. 6. Single-particle wave function $\varphi(k)$ in k space (left), for r space $\tilde{\varphi}(r)$ (middle), and occupation numbers (right) at $\mu = -5.26$ (top), -1.63 (middle), and 0.55 (bottom). The r-space wave function $\tilde{\varphi}(r)$ is derived from the Fourier transform of $\varphi(k)$ by $\tilde{\varphi}(r) = \int d^3k e^{i\vec{k}\cdot\vec{r}}\varphi(k)/(2\pi)^3$. The dashed line in the left panels correspond to the Gaussian with same norm and rms momentum as $\varphi(k)$.

In Fig. 5, we show the level density at zero temperature [$f(\omega) = \theta(-\omega)$], where it is calculated with the proton mass $m = 938.27$ MeV (natural unit). Two cases have to be considered, chemical potential μ positive or negative. In the latter case, we have binding of the quartet. Let us first discuss the case $\mu > 0$. We remark that in this case, the 3h level density goes through zero at $\omega = 0$, that is, just in the region where the quartet correlations should appear. This is a strong difference with the pairing case where the 1h level density does not feel any influence from the medium and, therefore, the corresponding level density varies (neglecting the mean field for the sake of the argument) as in free space with the square root of energy. In particular, this means that the level density is *finite* at the Fermi level. This is a dramatic difference with the quartet case and explains why Cooper pairs can strongly overlap whereas for quartets this is impossible. We also point out that the 3h level density is just the mirror to the 3p level density, which has been discussed in [29].

For the case where $\mu < 0$, there is nothing very special, besides the fact that it only is nonvanishing for negative values of ω and that the upper boundary is given by $\omega = 3\mu$. Therefore, the level density of Eq. (29) is zero for $\omega > 3\mu$.

VI. RESULTS AND DISCUSSION

At first, let us mention that in this pilot application of our self-consistent quartet theory, we only consider the zero-temperature case. As a definite physical example, we treat the case of nuclear physics with the particularly strongly bound quartet, the α particle. It should be pointed out, however, that if scaled appropriately, all energies and lengths can be transformed to other physical systems. For the nuclear case, it is convenient to measure energies in in Fermi energies $\varepsilon_F = 35$ MeV and lengths in inverse Fermi momentum $k_F^{-1} = 1.35^{-1}$ fm.

To determine the order parameter, the calculation iterates in the following cycle:

(i) Fix a chemical potential μ.
(ii) Give an initial trial order parameter $\varphi(k)$.
(iii) Calculate the mass operator $M^{\text{quartet}}(k, \omega)$ of Eq. (21) with $\varphi(k)$.
(iv) Calculate the occupation numbers $\rho(k)$ with $M^{\text{quartet}}(k, \omega)$ from Eq. (23).
(v) By substituting $\varphi(k)$ and $\rho(k)$ into Eqs. (26) and (27), derive the "new" single-particle wave function $\varphi(k)$ from

$$\varphi(k) = \frac{-3\mathcal{B}(k)}{\mathcal{A}(k) + 3\mathcal{C}(k)}. \tag{35}$$

(vi) Quit the cycle once $\varphi(k)$ has converged; otherwise, go to (iii).

The single-particle wave functions and occupation numbers obtained from this cycle are shown in Fig. 6. We take $\lambda = -992$ MeV fm^3 and $b = 1.43$ fm^{-1} to get the binding energy of the free α-particle (-28.3 MeV) and its radius (1.7 fm). We also insert the Gaussian wave function with same rms momentum as the single-particle wave function on the left in Fig. 6. As shown in Fig. 6, the single-particle wave function is sharper than a Gaussian. There is the term $\mathcal{A}(k)$ of Eq. (25) in the denominator of $\varphi(k)$ in Eq. (35), and $\mathcal{A}(k)$ involves the factor $[k^2/(2m) - 4\mu]$. Hence, $\varphi(k)$ is closer to a Lorentzian than to a Gaussian [1].

We could not obtain a convergent wave function for $\mu > 0.55$ MeV. This difficulty is of the same origin as in the case of our calculation of the critical temperature for α-particle condensation. This stems from the fact that for larger positive values of the chemical potential, the denominator of $\varphi(k)$ in Eq. (35) at a certain value of k becomes zero, while the numerator is finite. In the case of pair condensation, as shown in Eq. (4), both the denominator and numerator become zero at the same value of k, a further crucial difference between the quartet and pairing cases. In the right-hand panels of Fig. 6, we also show the corresponding occupation numbers. We see that they are very small. However, they increase for increasing values of the chemical potential. For $\mu = 0.55$ MeV, the maximum of the occupation still only attains 0.35, which is far away from the saturation value of 1. What really happens for larger values of the chemical potential is unclear. Surely, as discussed in Sec. V, the situation for the quartet case is completely different from the standard pairing case. This is because, as already mentioned, the 3h level density goes through zero at $\omega = 0$, that is, just at the place where the quartet correlation should build up for positive values of μ. Because of this fact, the inhibition to go into the positive μ regime is here even stronger than in the case of the critical temperature [21].

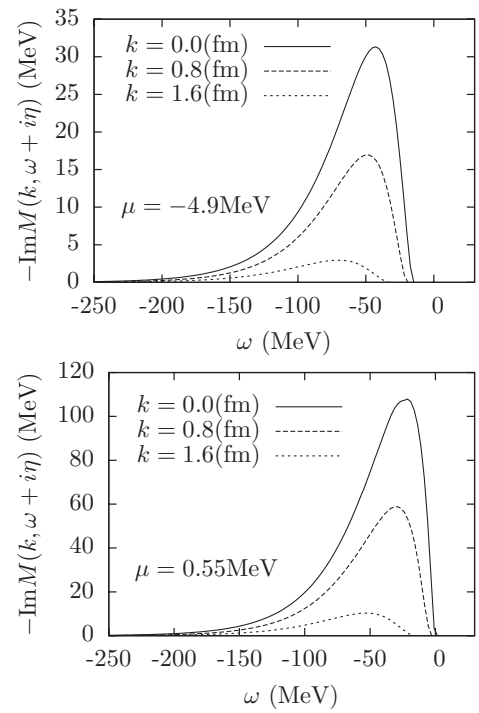

FIG. 7. $-\mathrm{Im}M^{\text{quartet}}(k_1, \omega + i\eta)$ in Eq. (22) as a function of ω for $\mu = -4.9$ MeV (left) and for $\mu = 0.55$ MeV (right) at zero temperature.

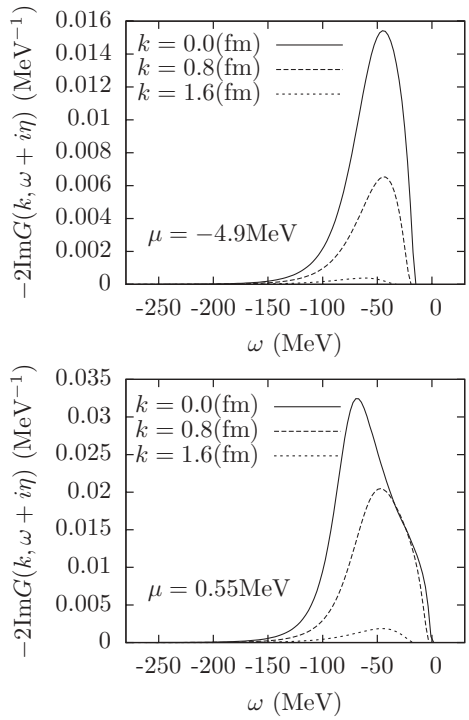

FIG. 8. $-2\mathrm{Im}G(k,\omega+i\eta)$ in Eq. (23) as function of ω for $\mu = -4.9$ MeV (top) and for $\mu = 0.55$ MeV (bottom) at zero temperature.

The situation in the quartet case is also much different, as the the 3h GF produces a considerable imaginary part of the mass operator. Figure 7 shows the imaginary part of the approximate quartet mass operator of Eq. (21) for $\mu < 0$ and $\mu > 0$. These large values of the damping rate imply a strong violation of the quasiparticle picture. In Fig. 8, we show the spectral function of the single-particle GF. Contrary to the pairing case with its sharp quasiparticle pole, we here only find a very broad distribution, implying that the quasiparticle picture is completely destroyed. How to formulate a theory that goes continuously from the quartet case into the pairing case is an open question. One solution could be to start right from the beginning with an in-medium four-body equation that contains a superfluid phase. When the quartet phase disappears, the superfluid phase may remain. Such investigations shall be done in the future.

VII. CONCLUSION

We formulated the gap equation for quartetting in fermion systems in analogy to the BCS gap equation. The mass operator of quartet-BEC with effective four-body vertices and in-medium four-body Schrödinger equation was derived with the Dyson equation approach to correlation functions. However, the full expression of the quartet mass operator is too complicated to be evaluated numerically in a direct manner. The biggest problem stems from the many-dimensional integrals over momenta. We, therefore, introduced some reasonable approximations and reduced the complexity considerably. A feature of great help is that the final answer is independent of the strength of the vertex function, probably making our approximation quite reliable. In our calculation, we also applied the same mean-field ansatz projected on zero total momentum, which was successful in our previous calculation of the critical temperature [21]. This feature, of course, reduces the numerical effort tremendously, because only a single $0S$ wave function has to be determined self-consistently by iteration.

In this pilot work with an application to nuclear physics, we showed results only at zero temperature; however, the formalism we presented is at finite temperature.

We think that the results are of general validity and show qualitatively very distinct features from the pairing case. For example, no well-defined quasiparticles occur in the case of quartets. This is because the quartet order parameter in the single-particle mass operator goes along with the level density of three uncorrelated holes. Only the total momentum of the three holes is well defined and equal to the time-reversed momentum of the incoming particle. The relative momenta of the three holes have to be integrated over, yielding a strong imaginary part of the mass operator and smoothing out any individual single-particle structure. Another remarkable feature already encountered in our previous work in Ref. [21] is that the self-consistent solution seems to exist only from negative chemical potential until around zero (i.e., from the BEC) or strong coupling region until crossover region. Once one goes to positive μ's, the solution breaks down. This effect is even more pronounced here than it was in our study [21] for the critical temperature. This can be traced back to the fact that the 3h level density goes through zero at 3μ for $\mu > 0$, that is, just at the place where the quartet correlations should occur. Actually, this feature is present for all multiparticle, multihole level densities. The only exception is the single-particle level density, which is finite at the Fermi level. This unique feature makes that pairing also unique and, for instance, allows for a weak coupling situation with a coherence length of the pair orders of magnitude larger than the interparticle distance. How to formulate a more general theory that continuously goes from the quartet case to the pairing case is an open problem.

ACKNOWLEDGMENTS

PS thanks M. Urban for useful discussions. This work was supported by the Deutsche Forschungsgemeinschaft (DFG) Grant No. RO905/29-1.

APPENDIX A: DYSON EQUATIONS FOR MULTIPARTICLE, MULTIHOLE GREEN FUNCTIONS

We review the basic formulation used in the present work. We here extend the approach for real-time GFs at zero temperature in Ref. [30] to real-time GFs at finite temperature [26,31].

The Hamiltonian in a fermion system with two-body interaction is

$$K = H - \mu N = T + V - \mu N = \sum_{1} \varepsilon_1 c_1^\dagger c_1 + \frac{1}{4} \sum_{1234} \bar{v}_{12,34} c_1^\dagger c_2^\dagger c_4 c_3. \quad \text{(A1)}$$

The $c_1, c_1^\dagger$ are fermion annihilation and creation operators with an arbitrary quantum number 1.

A real-time multiparticle, multihole GF at a finite temperature is defined by

$$G^{(i\mathrm{p}j\mathrm{h})}_{\alpha;\alpha'}(t-t') = \begin{cases} -i\langle T(A_\alpha(t)A^\dagger_{\alpha'}(t'))\rangle & \text{(chronological)} \\ -i\theta(t-t')\langle [A_\alpha(t), A^\dagger_{\alpha'}(t')]_\pm\rangle & \text{(retarded)} \end{cases} \tag{A2}$$

where $\langle\cdots\rangle$ means the thermal average, T is the time ordering operator, A_α is an arbitrary operator consisting of individual fermion operators c_1 and $c_1^\dagger$, and $[\ldots,\ldots]_\pm$ is the anticommutator or commutator. The time dependence of the operators is given in the Heisenberg picture $A_\alpha(t) = e^{iKt}A_\alpha e^{-iKt}$.

Note that although we treat chronological GFs here, the change to retarded, advanced, and Matsubara GFs goes as usual [26]. When we go from time space to Fourier space, we always go over to retarded GFs without mentioning it explicitly.

The superscript $(i\mathrm{p}j\mathrm{h})$ in Eq. (A2) means i-particle j-hole GF, where i (j) is the number of the annihilation (creation) operators in A_α, for example, $G^{(1\mathrm{p})}_{1;1'}(t-t') = -i\langle T(c_1(t)c^\dagger_{1'}(t'))\rangle$ and $G^{(1\mathrm{p}1\mathrm{h})}_{1,2;1',2'}(t-t') = -i\langle T((c^\dagger_2c_1)_t(c^\dagger_{1'}c_{2'})_{t'})\rangle$ with $(c^\dagger_2c_1)_t = c^\dagger_2(t)c_1(t)$.

The Dyson equation for the $i\mathrm{p}j\mathrm{h}$ GF is [30]

$$\left(i\frac{\partial}{\partial t} - \varepsilon_\alpha\right) G^{(i\mathrm{p}j\mathrm{h})}_{\alpha;\alpha'}(t-t') = \delta(t-t')\mathcal{N}_{\alpha;\alpha'} + \sum_\beta M^0_{\alpha;\beta}G^{(i\mathrm{p}j\mathrm{h})}_{\beta;\alpha'}(t-t') + \sum_\beta\int dt'' M_{\alpha;\beta}(t-t'')G^{(i\mathrm{p}j\mathrm{h})}_{\beta;\alpha'}(t''-t'), \tag{A3}$$

with

$$M^0_{\alpha;\alpha'} = \sum_\beta\langle[[A_\alpha, V]_-, A^\dagger_\beta]_\pm\rangle\mathcal{N}^{-1}_{\beta;\alpha'} \tag{A4}$$

$$M_{\alpha;\alpha'}(t-t') = -i\sum_\beta\langle T([A_\alpha(t), V]_-[V, A^\dagger_\beta(t')]_-)\rangle_{\mathrm{irr.}}\mathcal{N}^{-1}_{\beta;\alpha'}, \tag{A5}$$

$$\mathcal{N}_{\alpha;\alpha'} = \langle[A_\alpha, A^\dagger_{\alpha'}]_\pm\rangle, \tag{A6}$$

where ε_α is defined by $[A_\alpha, T-\mu N]_- = \varepsilon_\alpha A_\alpha$, and $\mathcal{N}^{-1}_{\alpha;\alpha'}$ is the inverse of the matrix $\mathcal{N}_{\alpha;\alpha'}$.

According to the time dependence, we call $M^0_{\alpha;\alpha'}$ static mass operator and $M_{\alpha;\alpha'}(t-t')$ dynamical mass operator.

Because $[A_\alpha(t), V]_-$ is the operator A_α augmented by one annihilation and one creation operator, $\langle T([A_\alpha(t), V]_-[V, A^\dagger_\beta(t'')]_-)\rangle_{\mathrm{irr.}}$ becomes a $(i+1)\mathrm{p}(j+1)\mathrm{h}$ GF in the dynamical mass of Eq. (A5). The index "irr." in Eq. (A5) stands for the mass operator being irreducible with respect to a cut of $i\mathrm{p}j\mathrm{h}$ lines [24].

From the Dyson equation of Eq. (A3), we can see that the Fourier transform of the bare $i\mathrm{p}j\mathrm{h}$ GF is

$$G^{0(i\mathrm{p}j\mathrm{h})}_{\alpha;\alpha'}(\omega) = \frac{\mathcal{N}_{\alpha;\alpha'}}{\omega-\varepsilon_\alpha}. \tag{A7}$$

APPENDIX B: QUARTET MASS OPERATOR

Here we derive the quartet mass operator of Eq. (8) shown in Sec. III.

Notice that we use the summation convention for repeated indices and neglect all terms except the ones that are associated with the quartet order parameters.

From Eq. (A3), the Dyson equation for the 1p GF is [24]

$$\left(i\frac{\partial}{\partial t} - \varepsilon_1\right) G^{(1\mathrm{p})}_{1;2}(t_1-t_2) = \delta_{12}\delta(t_1-t_2) + \int dt_3 M^{(1\mathrm{p})}_{1;3}(t_1-t_3)G^{(1\mathrm{p})}_{3;2}(t_3-t_2). \tag{B1}$$

The Fourier transform yields

$$(\omega-\varepsilon_1)G^{(1\mathrm{p})}_{1;2}(\omega) = \delta_{12} + M^{(1\mathrm{p})}_{1;3}(\omega)G^{(1\mathrm{p})}_{3;2}(\omega) \tag{B2}$$

with

$$M^{(1\mathrm{p})}_{1;2}(\omega) = \tfrac{1}{2}\bar{v}_{1z_1,a_1a_1'}G^{(2\mathrm{p}1\mathrm{h})\mathrm{irr.}}_{a_1a_1',z_1;a_2a_2',z_2}(\omega)\tfrac{1}{2}\bar{v}_{2z_2,a_2a_2'}. \tag{B3}$$

Therefore,

$$G^{(1\mathrm{p})}_{1;2}(\omega) = G^{0(1\mathrm{p})}_{1;2}(\omega) + G^{0(1\mathrm{p})}_{1;3}(\omega)M^{(1\mathrm{p})}_{3;4}(\omega)G^{(1\mathrm{p})}_{4;2}(\omega), \tag{B4}$$

where

$$G^{0(1\mathrm{p})}_{1;2}(\omega) = \frac{\delta_{12}}{\omega-\varepsilon_1}. \tag{B5}$$

For the Dyson equation of the 2p1h GF, one obtains

$$[\omega-(\varepsilon_{a_1}+\varepsilon_{a_1'}-\varepsilon_{z_1})]G^{(2\mathrm{p}1\mathrm{h})}_{a_1a_1',z_1;a_2a_2',z_2}(\omega) = \mathcal{N}_{a_1a_1',z_1;a_2a_2',z_2} + M^{(2\mathrm{p}1\mathrm{h})}_{a_1a_1',z_1;a_3a_3',z_3}(\omega)G^{(2\mathrm{p}1\mathrm{h})}_{a_3a_3',z_3;a_2a_2',z_2}(\omega), \tag{B6}$$

where

$$\begin{aligned} &M^{(2\mathrm{p}1\mathrm{h})}_{a_1a_1',z_1;a_2a_2',z_2}(\omega) \\ &= \left[\tfrac{1}{2}\bar{v}_{a_1y_1,b_1b_1'}\delta_{z_1y_1'}\delta_{a_1'b_1''} + \tfrac{1}{2}\bar{v}_{a_1'y_1',b_1b_1'}\delta_{z_1y_1}\delta_{a_1b_1''}\right. \\ &\quad \left. - \tfrac{1}{2}\bar{v}_{z_1b_1'',y_1y_1'}\delta_{a_1b_1}\delta_{a_1'b_1'}\right]G^{(3\mathrm{p}2\mathrm{h})\mathrm{irr.}}_{b_1b_1'b_1'',y_1y_1';b_2b_2'b_2'',y_2y_2'}(\omega) \\ &\quad \times\left[\tfrac{1}{2}\bar{v}_{a_3y_2,b_2b_2'}\delta_{z_3y_2'}\delta_{a_3'b_2''} + \tfrac{1}{2}\bar{v}_{a_3'y_2',b_2b_2'}\delta_{z_3y_2}\delta_{a_3b_3''}\right. \\ &\quad \left. - \tfrac{1}{2}\bar{v}_{z_3b_2'',y_2y_2'}\delta_{a_3b_2}\delta_{a_3'b_2'}\right]\mathcal{N}^{-1}_{a_3a_3',z_3;a_2a_2',z_2} \end{aligned} \tag{B7}$$

and

$$\mathcal{N}_{a_1a_1',z_1;a_2a_2',z_2} = \left\langle\left[c^\dagger_{z_1}c_{a_1'}c_{a_1}, c^\dagger_{a_2}c^\dagger_{a_2'}c_{z_2}\right]_+\right\rangle. \tag{B8}$$

Therefore,

$$\begin{aligned} &G^{(2\mathrm{p}1\mathrm{h})}_{a_1a_1',z_1;a_2a_2',z_2}(\omega) \\ &= G^{0(2\mathrm{p}1\mathrm{h})}_{a_1a_1',z_1;a_2a_2',z_2}(\omega) + G^{0(2\mathrm{p}1\mathrm{h})}_{a_1a_1',z_1;a_3a_3',z_3}(\omega)\mathcal{N}^{-1}_{a_3a_3',z_3;a_4a_4',z_4} \\ &\quad \times M^{(2\mathrm{p}1\mathrm{h})}_{a_4a_4',z_4;a_5a_5',z_5}(\omega)G^{(2\mathrm{p}1\mathrm{h})}_{a_5a_5',z_5;a_2a_2',z_2}(\omega), \end{aligned} \tag{B9}$$

with

$$G^{0(2\mathrm{p}1\mathrm{h})}_{a_1a_1',z_1;a_2a_2',z_2}(\omega) = \frac{\mathcal{N}_{a_1a_1',z_1;a_2a_2',z_2}}{\omega-\left(\varepsilon_{a_1a_1'}-\varepsilon_{z_1}\right)} \tag{B10}$$

and

$$\mathcal{N}_{a_1a_1',z_1;a_3a_3',z_3}\mathcal{N}^{-1}_{a_3a_3',z_3;a_2a_2',z_2} = \delta_{a_1a_2}\delta_{a_1'a_2'}\delta_{z_1z_2}, \tag{B11}$$

where $\varepsilon_{ij\ldots} = \varepsilon_i + \varepsilon_j + \cdots$ in (B10).

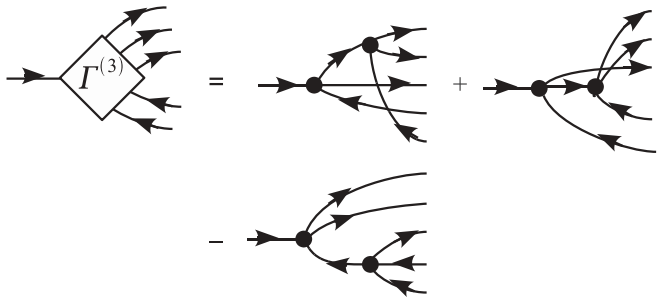

FIG. 9. Graphical representation of $\Gamma^{(3)}$ in Eq. (B13). The dots is represent the two-body interaction.

Substituting the 2p1h GF of Eq. (B9) into the mass operator of Eq. (B3), we obtain

$$M^{(1p)}_{1;2}(\omega) = \Gamma^{(3)}_{1y_1y_1',b_1b_1'b_1''}(\omega) G^{(3p2h)irr.}_{b_1b_1'b_1'',y_1y_1';b_2b_2'b_2'',y_2y_2'}(\omega) \times \Gamma^{(3)*}_{2y_2y_2',b_2b_2'b_2''}(\omega), \tag{B12}$$

where

$$\Gamma^{(3)}_{1y_1y_1',b_1b_1'b_1''}(\omega) = \tfrac{1}{2}\bar{v}_{1z_1,a_1a_1'} G^{0(2p1h)}_{a_1a_1',z_1;a_3a_3',z_3}(\omega)\mathcal{N}^{-1}_{a_3a_3',z_3;a_4a_4',z_4} \times \left[\tfrac{1}{2}\bar{v}_{a_4y_1,b_1b_1'}\delta_{z_1y_1'}\delta_{a_4'b_1''} + \tfrac{1}{2}\bar{v}_{a_4'y_1',b_1b_1'}\delta_{z_1y_1}\delta_{a_4b_1''} - \tfrac{1}{2}\bar{v}_{z_4b_1'',y_1y_1'}\delta_{a_4b_1}\delta_{a_4'b_1'}\right]. \tag{B13}$$

This three body vertex is graphically displayed in Fig. 9. In Eq. (B12), we omitted the term derived from the first term of the right-hand side of Eq. (B9) because it is disconnected with the quartet order parameter. In the effective three-body vertex $\Gamma^{(3)}$ of Eq. (B13), we give not the exact 2p1h GF but the free one, as we only consider in this work the lowest order approximation, though the exact 2p1h GF figures, in principle, in the right vertex $\Gamma^{(3)}$ of Eq. (B13) by substituting Eq. (B9) into Eq. (B3). In Eq. (B13), using Eqs. (B10) and (B11), we obtain

$$G^{0(2p1h)}_{a_1a_1',z_1;a_3a_3',z_3}(\omega)\mathcal{N}^{-1}_{a_3a_3',z_3;a_4a_4',z_4} = \frac{\delta_{a_1a_4}\delta_{a_1'a_4'}\delta_{z_1z_4}}{\omega - \varepsilon_{a_1a_1'} + \varepsilon_{z_1}}, \tag{B14}$$

and thus Eq. (B13) is consistent with Eq. (11).

Furthermore, the Dyson equation for 3p2h GF is

$$\left[\omega - \left(\varepsilon_{b_1b_1'b_1''} - \varepsilon_{y_1y_1'}\right)\right] G^{(3p2h)}_{b_1b_1'b_1'',y_1y_1';b_2b_2'b_2'',y_2y_2'}(\omega) = \mathcal{N}_{b_1b_1'b_1'',y_1y_1';b_2b_2'b_2'',y_2y_2'} + M^{(3p2h)}_{b_1b_1'b_1'',y_1y_1';b_3b_3'b_3'',y_3y_3'}(\omega) \times G^{(3p2h)}_{b_3b_3'b_3'',y_3y_3';b_2b_2'b_2'',y_2y_2'}(\omega). \tag{B15}$$

The mass operator is then given by

$$\begin{aligned} M^{(3p2h)}_{b_1b_1'b_1'',y_1y_1';b_2b_2'b_2'',y_2y_2'}(\omega) &= \left[\tfrac{1}{2}\bar{v}_{b_1x_1'',c_1c_1'''}\delta_{y_1x_1}\delta_{y_1'x_1'}\delta_{b_1'c_1'}\delta_{b_1''c_1''} + \tfrac{1}{2}\bar{v}_{b_1'x_1'',c_1'c_1'''}\delta_{y_1x_1}\delta_{y_1'x_1'} \right. \\ &\times \delta_{b_1c_1}\delta_{b_1''c_1''} + \tfrac{1}{2}\bar{v}_{b_1''x_1'',c_1''c_1'''}\delta_{y_1x_1}\delta_{y_1'x_1'}\delta_{b_1c_1}\delta_{b_1'c_1'} \\ &- \tfrac{1}{2}\bar{v}_{y_1c_1''',x_1x_1''}\delta_{y_1'x_1'}\delta_{b_1c_1}\delta_{b_1'c_1'}\delta_{b_1''c_1''} - \tfrac{1}{2}\bar{v}_{y_1'c_1''',x_1'x_1''} \\ &\times \delta_{y_1x_1}\delta_{b_1c_1}\delta_{b_1'c_1'}\delta_{b_1''c_1''}\left.\right] G^{(4p3h)irr.}_{c_1c_1'c_1''c_1''',x_1x_1'x_1'';c_2c_2'c_2''c_2''',x_2x_2'x_2''}(\omega) \\ &\times \left[\tfrac{1}{2}\bar{v}_{b_3x_2'',c_2c_2'''}\delta_{y_3x_2}\delta_{y_3'x_2'}\delta_{b_3'c_2'}\delta_{b_3''c_2''} + \tfrac{1}{2}\bar{v}_{b_3'x_2'',c_2'c_2'''}\delta_{y_3x_2}\right. \\ &\times \delta_{y_3'x_2'}\delta_{b_3c_2}\delta_{b_3''c_2''} + \tfrac{1}{2}\bar{v}_{b_3''x_2'',c_2''c_2'''}\delta_{y_3x_2}\delta_{y_3'x_2'}\delta_{b_3c_2}\delta_{b_3'c_2'} \\ &- \tfrac{1}{2}\bar{v}_{y_3c_2''',x_2x_2''}\delta_{y_3'x_2'}\delta_{b_3c_2}\delta_{b_3'c_2'}\delta_{b_3''c_2''} - \tfrac{1}{2}\bar{v}_{y_3'c_2''',x_2'x_2''}\delta_{y_3x_2}\delta_{b_3c_2} \\ &\times \left.\delta_{b_3'c_2'}\delta_{b_3''c_2''}\right]\mathcal{N}^{-1}_{b_3b_3'b_3'',y_3y_3';b_2b_2'b_2'',y_2y_2'}, \end{aligned} \tag{B16}$$

and

$$\mathcal{N}_{b_1b_1'b_1'',y_1y_1';b_2b_2'b_2'',y_2y_2'} = \left\langle\left[c^\dagger_{y_1}c^\dagger_{y_1'}c_{b_1''}c_{b_1'}c_{b_1}, c^\dagger_{b_1}c^\dagger_{b_1'}c^\dagger_{b_1''}c_{y_1'}c_{y_1}\right]_+\right\rangle. \tag{B17}$$

Therefore, one obtains for the 3p2h GF

$$\begin{aligned} G^{(3p2h)}_{b_1b_1'b_1'',y_1y_1';b_2b_2'b_2'',y_2y_2'}(\omega) &= G^{0(3p2h)}_{b_1b_1'b_1'',y_1y_1';b_2b_2'b_2'',y_2y_2'}(\omega) + G^{0(3p2h)}_{b_1b_1'b_1'',y_1y_1';b_3b_3'b_3'',y_3y_3'}(\omega) \\ &\times \mathcal{N}^{-1}_{b_3b_3'b_3'',y_3y_3';b_4b_4'b_4'',y_4y_4'} M^{(3p2h)}_{b_4b_4'b_4'',y_4y_4';b_5b_5'b_5'',y_5y_5'}(\omega) \\ &\times G^{(3p2h)}_{b_5b_5'b_5'',y_5y_5';b_2b_2'b_2'',y_2y_2'}(\omega), \end{aligned} \tag{B18}$$

where

$$G^{0(3p2h)}_{b_1b_1'b_1'',y_1y_1';b_2b_2'b_2'',y_2y_2'}(\omega) = \frac{\mathcal{N}_{b_1b_1'b_1'',y_1y_1';b_2b_2'b_2'',y_2y_2'}}{\omega - \left(\varepsilon_{b_1b_1'b_1''} - \varepsilon_{y_1y_1'}\right)}. \tag{B19}$$

By substituting 3p2h GF of (B18) into the mass operator of Eq. (B12), we get

$$M^{(1p)}_{1;2}(\omega) = \Gamma^{(4)}_{1x_1x_1'x_1'',c_1c_1'c_1''c_1'''}(\omega) G^{(4p3h)irr.}_{c_1c_1'c_1''c_1''',x_1x_1'x_1'';c_2c_2'c_2''c_2''',x_2x_2'x_2''}(\omega) \times \Gamma^{(4)*}_{2x_2x_2'x_2'',c_2c_2'c_2''c_2'''}(\omega), \tag{B20}$$

with

$$\begin{aligned} \Gamma^{(4)}_{1x_1x_1'x_1'',c_1c_1'c_1''c_1'''}(\omega) &= \Gamma^{(3)}_{1y_1y_1',b_1b_1'b_1''}(\omega) G^{0(3p2h)}_{b_1b_1'b_1'',y_1y_1';b_3b_3'b_3'',y_3y_3'}(\omega) \\ &\times \mathcal{N}^{-1}_{b_3b_3'b_3'',y_3y_3';b_4b_4'b_4'',y_4y_4'}\left[\tfrac{1}{2}\bar{v}_{b_4x_1'',c_1c_1'''}\delta_{y_4x_1}\delta_{y_4'x_1'}\delta_{b_4'c_1'}\delta_{b_4''c_1''}\right. \\ &+ \tfrac{1}{2}\bar{v}_{b_4'x_1'',c_1'c_1'''}\delta_{y_4x_1}\delta_{y_4'x_1'}\delta_{b_4c_1}\delta_{b_4''c_1''} + \tfrac{1}{2}\bar{v}_{b_4''x_1'',c_1''c_1'''}\delta_{y_4x_1} \\ &\times \delta_{y_4'x_1'}\delta_{b_4c_1}\delta_{b_4'c_1'} - \tfrac{1}{2}\bar{v}_{y_4c_1''',x_1x_1''}\delta_{y_4'x_1'}\delta_{b_4c_1}\delta_{b_4'c_1'}\delta_{b_4''c_1''} \\ &- \left.\tfrac{1}{2}\bar{v}_{y_4'c_1''',x_1'x_1''}\delta_{y_4x_1}\delta_{b_4c_1}\delta_{b_4'c_1'}\delta_{b_4''c_1''}\right]. \end{aligned} \tag{B21}$$

Here we also omitted the terms associated with the first term at the right-hand side of Eq. (B18) because it is disconnected with the quartet order parameter. Besides, we introduced the free 3p2h GF in $\Gamma^{(4)}$ of (B21) for the same reason, as this was done in Eqs. (B12) and (B13). The graphical representation of $\Gamma^{(4)}$ is shown in Fig. 10.

The 4p3h GF can, for our purpose of α-particle condensation, be approximately decomposed into the order parameter and the free three-body GF as follows (in analogy to what is done in the pairing case):

$$\begin{aligned} G^{(4p3h)}_{c_1c_1'c_1''c_1''',x_1x_1'x_1'';c_2c_2'c_2''c_2''',x_2x_2'x_2''}(t_1 - t_2) &= -i\left\langle T\left(c^\dagger_{x_1}c^\dagger_{x_1'}c^\dagger_{x_1''}c_{c_1'''}c_{c_1''}c_{c_1'}c_{c_1}\right)_{t_1}\left(c^\dagger_{c_2}c^\dagger_{c_2'}c^\dagger_{c_2''}c^\dagger_{c_2'''}c_{x_2''}c_{x_2'}c_{x_2}\right)_{t_2}\right\rangle \\ &= -i\left\langle T\left(c_{c_1'''}c_{c_1''}c_{c_1'}c_{c_1}\right)_{t_1}\right\rangle\left\langle T\left(c^\dagger_{c_2}c^\dagger_{c_2'}c^\dagger_{c_2''}c^\dagger_{c_2'''}\right)_{t_2}\right\rangle \\ &\times \left\langle T\left(c^\dagger_{x_1}c^\dagger_{x_1'}c^\dagger_{x_1''}\right)_{t_1}\left(c_{x_2''}c_{x_2'}c_{x_2}\right)_{t_2}\right\rangle \\ &= \left\langle c_{c_1'''}c_{c_1''}c_{c_1'}c_{c_1}\right\rangle\left\langle c^\dagger_{c_2}c^\dagger_{c_2'}c^\dagger_{c_2''}c^\dagger_{c_2'''}\right\rangle G^{0(3h)}_{x_1x_1'x_1'';x_2x_2'x_2''}(t_1 - t_2) \end{aligned} \tag{B22}$$

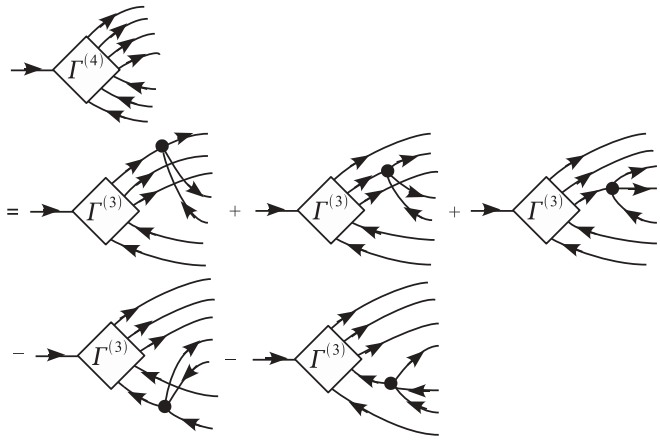

FIG. 10. Graphical representation of $\Gamma^{(4)}$ in Eq. (B21).

The Fourier transform is

$$G^{(4p3h)}_{c_1c_1'c_1''c_1''',x_1x_1'x_1'';c_2c_2'c_2''c_2''',x_2x_2'x_2''}(\omega) = \langle c_{c_1'''}c_{c_1''}c_{c_1'}c_{c_1}\rangle\langle c^\dagger_{c_2}c^\dagger_{c_2'}c^\dagger_{c_2''}c^\dagger_{c_2'''}\rangle G^{0(3h)}_{x_1x_1'x_1'';x_2x_2'x_2''}(\omega). \quad \text{(B23)}$$

The free 3h GF is explicitly given by

$$G^{0(3h)}_{x_1x_1'x_1'';x_2x_2'x_2''}(\omega) = \frac{\bar f_{x_1}\bar f_{x_1'}\bar f_{x_1''} + f_{x_1}f_{x_1'}f_{x_1''}}{\omega + \varepsilon_{x_1x_1'x_1''}} P_{x_1x_1'x_1'';x_2x_2'x_2''}, \quad \text{(B24)}$$

with $P_{x_1x_1'x_1'';x_2x_2'x_2''}$ as in Eq. (9).

Therefore, Eq. (B23) becomes

$$G^{(4p3h)}_{c_1c_1'c_1''c_1''',x_1x_1'x_1'';c_2c_2'c_2''c_2''',x_2x_2'x_2''}(\omega) = \langle c_{c_1'''}c_{c_1''}c_{c_1'}c_{c_1}\rangle\langle c^\dagger_{c_2}c^\dagger_{c_2'}c^\dagger_{c_2''}c^\dagger_{c_2'''}\rangle \frac{\bar f_{x_1}\bar f_{x_1'}\bar f_{x_1''} + f_{x_1}f_{x_1'}f_{x_1''}}{\omega + \varepsilon_{x_1x_1'x_1''}} \times P_{x_1x_1'x_1'';x_2x_2'x_2''}. \quad \text{(B25)}$$

Finally, we obtain for the quartet mass operator

$$M^{\text{quartet}}_{1;2}(\omega) = \Gamma^{(4)}_{1x_1x_1'x_1'';c_1c_1'c_1''c_1'''}(\omega)\langle c_{c_1'''}c_{c_1''}c_{c_1'}c_{c_1}\rangle \times \frac{\bar f_{x_1}\bar f_{x_1'}\bar f_{x_1''} + f_{x_1}f_{x_1'}f_{x_1''}}{\omega + \varepsilon_{x_1x_1'x_1''}} P_{x_1x_1'x_1'';x_2x_2'x_2''} \times \langle c^\dagger_{c_2}c^\dagger_{c_2'}c^\dagger_{c_2''}c^\dagger_{c_2'''}\rangle\Gamma^{(4)*}_{2x_2x_2'x_2'';c_2c_2'c_2''c_2'''}(\omega). \quad \text{(B26)}$$

APPENDIX C: IN-MEDIUM QUARTET ORDER PARAMETER EQUATION

We here give a short derivation of the in-medium quartet order parameter equation. It is derived from the Dyson equation for 4p GF in static approximation of the mass operator. The Dyson equation for 4p GF derived from Eq. (A3) without dynamical mass operator is

$$\left(i\frac{\partial}{\partial t} - \varepsilon_{1234}\right) G^{(4p)}_{1234;1'2'3'4'}(t-t') = \mathcal{N}_{1234;1'2'3'4'} + V_{1234;1''2''3''4''}G^{(4p)}_{1234;1'2'3'4'}(t-t'), \quad \text{(C1)}$$

with, to lowest order in the interaction,

$$\begin{aligned} V_{1234;1'2'3'4'} &= \langle[[c_4c_3c_2c_1, V]_-, c^\dagger_{1''}c^\dagger_{2''}c^\dagger_{3''}c^\dagger_{4''}]_-\rangle\mathcal{N}^{-1}_{1''2''3''4'';1'2'3'4'} \\ &= \tfrac{1}{2}(1-\rho_1-\rho_2)\bar v_{12,1'2'}\delta_{33'}\delta_{44'} + \tfrac{1}{2}(1-\rho_1-\rho_3)\bar v_{13,1'3'} \times \delta_{22'}\delta_{44'} + \tfrac{1}{2}(1-\rho_1-\rho_4)\bar v_{14,1'4'}\delta_{22'}\delta_{33'} \\ &\quad + \text{permutations}, \end{aligned} \quad \text{(C2)}$$

where we approximated the correlation functions by factorizing them into products of single-particle occupation numbers.

The Fourier transform of 4p GF is

$$G^{(4p)}_{1234;1'2'3'4'}(\omega) = G^{0(4p)}_{1234;1'2'3'4'}(\omega) + G^{0(4p)}_{1234;1''2''3''4''}(\omega)\mathcal{N}^{-1}_{1''2''3''4'';5678} \times V_{5678;5'6'7'8'}G^{(4p)}_{5'6'7'8';1'2'3'4'}(\omega), \quad \text{(C3)}$$

where

$$G^{0(4p)}_{1234;1'2'3'4'}(\omega) = \frac{\mathcal{N}_{1234;1'2'3'4'}}{\omega - \varepsilon_{1234}}. \quad \text{(C4)}$$

From the spectral representation of the 4p GF, we retain only the ground state because of its condensate character. Therefore, at the ground-state pole (i.e., at $\omega = 0$), we obtain

$$\langle c_4c_3c_2c_1\rangle = -\frac{1}{\varepsilon_{1234}}V_{1234;1'2'3'4'}\langle c_{4'}c_{3'}c_{2'}c_{1'}\rangle. \quad \text{(C5)}$$

This equation corresponds to Eq. (4) in the pairing case.

APPENDIX D: APPROXIMATE MASS OPERATOR IN EQ. (17)

After the derivation of a single-particle mass operator containing the quartet condensate in Appendix B, we easily recognize that its expression, for instance, the vertex $\Gamma^{(4)}$ in Eqs. (10) and (11) [or (B13) and (B21)] is of considerable complexity, prohibitive for a direct numerical application, especially because of high-dimensional integrals. Therefore, we have to proceed to a quite intensive study of vertices, followed by reasonable approximations, to reduce drastically the numerical difficulty of the expressions.

A first purely formal simplification, which we introduce, is to consider only the trion case instead of the quartet case. Trions are fermions, and one would have to develop a whole proper philosophy to introduce an order parameter for trions. However, we ignore this difficulty here, proceed formally as if a trion order parameter existed in the same way as a quartet order parameter, and explain our strategy for this much simpler case. This can be done without loss of generality, and in the end we simply give our results for the quartet case, which can be derived in complete analogy to the trion case.

Let us, therefore, begin with the expression of the single-particle mass operator containing a "trion condensate," which analogously to Eq. (B26) is given by

$$M_{1;1'}(\omega) = \Gamma^{(3)}_{123;456}(\omega)\langle c_6c_5c_4\rangle\frac{\bar f_2\bar f_3 - f_2f_3}{\omega + \varepsilon_{23}}(\delta_{22'}\delta_{33'} - \delta_{23'}\delta_{32'})\langle c^\dagger_{4'}c^\dagger_{5'}c^\dagger_{6'}\rangle\Gamma^{(3)*}_{1'2'3';4'5'6'}(\omega), \quad \text{(D1)}$$

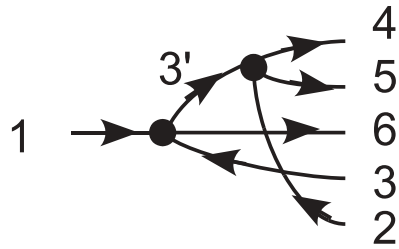

FIG. 11. Graphical expression of the first term on the right-hand side of Eq. (11).

with $\Gamma^{(3)}$ as the three-body vertex already given in Eq. (11) and derived in Eq. (B13). The first and rather obvious approximation we perform is to make $\Gamma^{(3)}$ instantaneous, that is, ω independent. A standard procedure for this is to put the vertex on the energy shell. This procedure is not always defined unambiguously. In the present case, one possibility certainly is to put in $\Gamma^{(3)}$, $\omega = -\varepsilon_{23}$, that is, the energy, where the mass operator (D1) is resonant.

Let us for the moment only investigate the first term on the right-hand side of Eq. (11) with this prescription. We obtain

$$\Gamma^{(3,1)}_{123;456}(\omega = -\varepsilon_{23}) = \frac{1}{4}\bar{v}_{13,3'6}\frac{1}{-\varepsilon_2 - \varepsilon_{3'} - \varepsilon_6}\bar{v}_{3'2,45}. \tag{D2}$$

A graphical interpretation of this term is given in Fig. 11.

This graph also can be interpreted as a particular second-order term of a three-body scattering process (123) → (456), graphically represented in Fig. 12.

The intermediate propagator between the two vertices is given by $1/(-\varepsilon_2 - \varepsilon_{3'} - \varepsilon_6)$ (the energies are given by the propagators, which are cut by the vertical line in Fig. 12). Therefore, we see that the static, on-shell part $\Gamma^{(3)}(\omega = -\varepsilon_{23})$ of Eq. (D1) can be interpreted as a second-order three-body scattering taken at $\omega = 0$, that is, in reality at three times the Fermi energy. This certainly is a reasonable reduction of the second-order process to a static vertex $\Gamma^{(3,1)}$.

Proceeding in the same way with the second term on the right-hand side of Eq. (11), we arrive at a second-order process analogous to the one of Fig. 12, as shown in Fig. 13. We see that Fig. 13 corresponds to Fig. 12 with particles 2 and 3 permuted.

Let us now consider the third term in Eq. (11). In analogy to processes of Figs. 12 and 13, this corresponds to the graph of Fig. 14.

If we interpret this third term also as a static second-order three-body process with an intermediate propagator $1/(-\varepsilon_1 - \varepsilon_{2'} - \varepsilon_6)$ at $\omega = 0$, contrary to the first and second

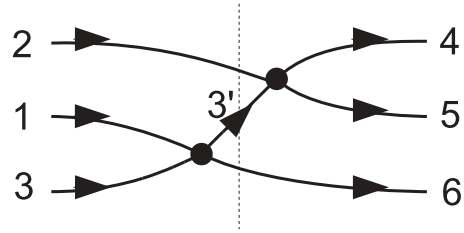

FIG. 12. Topologically same diagram as in Fig. 11.

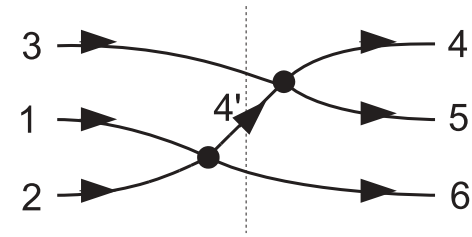

FIG. 13. Graphical expression of the second term on the right-hand side of Eq. (11).

terms of Eq. (11), we have to use as on-shell prescription in Eq. (11): $\omega = \varepsilon_1 + \varepsilon_4 + \varepsilon_5 + \varepsilon_6$. We thus suppose from now on that all vertices in $\Gamma^{(3)}$ are obtained from a second-order three-body scattering process at $\omega = 0$.

After these preliminary considerations, let us now introduce in a phenomenological intuitive way a single-particle mass operator containing a trion order parameter in a way analogous to the pairing case

$$M_{1;1'}(\omega) = \int \frac{d\omega'}{2\pi}\mathrm{Im}T_{123;1'2'3'}(\omega - \omega')G^0_{23,2'3'}(-\omega'), \tag{D3}$$

with

$$\mathrm{Im}T_{123;1'2'3'}(\omega) = -2\pi\delta(\omega)\bar{V}_{123;456}\psi^t_{456}\psi^{t*}_{4'5'6'}\bar{V}_{4'5'6';1'2'3'} \tag{D4}$$

and

$$\bar{V}_{123;1'2'3'} = \tfrac{1}{2}(\bar{v}_{12,1'2'}\delta_{33'} + \bar{v}_{13,1'3'}\delta_{22'} + \bar{v}_{23,2'3'}\delta_{11'}), \tag{D5}$$

where we abbreviated the order parameter as

$$\langle c_3 c_2 c_1\rangle = \psi^t_{123}. \tag{D6}$$

The three-body T-matrix (D4) in Eq. (D3) is contracted with the antisymmetrized 2h propagator

$$G^0_{23,2'3'}(-\omega) = -\frac{\bar{f}_2\bar{f}_3 - f_2 f_3}{\omega + \varepsilon_{23}}(\delta_{22'}\delta_{33'} - \delta_{23'}\delta_{32'}). \tag{D7}$$

With these definitions, Eqs. (D3)–(D7), we indeed see that the trion mass operator is constructed in full analogy to the one of the pairing case in Eq. (2). It is evident that in the quartet case we would define a four-body T matrix as

$$\mathrm{Im}T_{1234;1'2'3'4'}(\omega) = -2\pi\delta(\omega)\Delta_{1234}\Delta^*_{1'2'3'4'} \tag{D8}$$

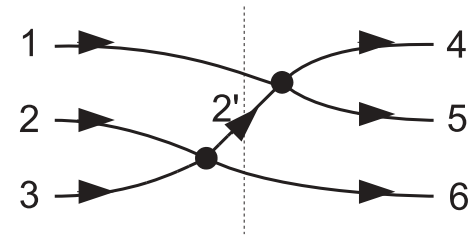

FIG. 14. Graphical expression of the third term on the right-hand side of Eq. (11).

with

$$\Delta_{1234;5678} = \bar{V}_{1234;5678}\langle c_8 c_7 c_6 c_5\rangle \tag{D9}$$

and

$$\bar{V}_{1234;1'2'3'4'} = \tfrac{1}{2}\bar{v}_{12;1'2'}\delta_{33'}\delta_{44'} + \tfrac{1}{2}\bar{v}_{13;1'3'}\delta_{22'}\delta_{44'} + \text{permutations} \tag{D10}$$

and contract it with a 3h GF.

Let us now investigate whether we can make contact of the mass operator in Eq. (D3) with the one of Eq. (D1). To this purpose, let us use in Eq. (D4) the equation for the trion order parameter, which in analogy to (C3) is given by

$$\psi^t_{123} = -\frac{1}{\varepsilon_{123}}\Big[(1-\rho_1-\rho_2)\frac{1}{2}\bar{v}_{12,1'2'}\delta_{33'} + (1-\rho_1-\rho_3) \times \frac{1}{2}\bar{v}_{13,1'3'}\delta_{22'} + (1-\rho_2-\rho_3)\frac{1}{2}\bar{v}_{23,2'3'}\delta_{11'}\Big]\psi^t_{1'2'3'} \tag{D11}$$

and investigate for the moment only the expression corresponding to the second term on the right-hand side of Eq. (D5). We obtain

$$\frac{1}{2}\bar{v}_{13,46}\delta_{25}\psi^t_{456} = \frac{1}{2}\bar{v}_{13,46}\delta_{25}\frac{1}{-\varepsilon_{123}}\Big[(1-\rho_4-\rho_5)\frac{1}{2}\bar{v}_{45,4'5'}\delta_{66'} + (1-\rho_4-\rho_6)\frac{1}{2}\bar{v}_{46,4'6'}\delta_{55'} + (1-\rho_5-\rho_6)\frac{1}{2}\bar{v}_{56,5'6'}\delta_{44'}\Big]\psi^t_{4'5'6'}. \tag{D12}$$

We notice some similarity with the second-order vertex (D1). The difference stems from the presence of the occupation numbers ρ_i in Eq. (D12) and from the fact that there is more than one term. In principle, the occupation numbers are the correlated ones. In the main part of this article, we have seen that our theory is practically only valid for $\mu < 0$, implying that the occupation numbers remain small; see Fig. 6. We therefore can neglect the occupation numbers in Eq. (D12) to good approximation (for the $\mu < 0$ regime). Then, we can read off a vertex from Eq. (D12) of the following form:

$$\tilde{\Gamma}^{(3,2)}_{123;456} = \frac{1}{4}\bar{v}_{13,3'6}\frac{1}{-\varepsilon_{23'6}}\bar{v}_{3'2,45} + \frac{1}{4}\bar{v}_{13,3'6'}\delta_{25}\frac{1}{-\varepsilon_{23'6'}}\bar{v}_{3'6',46} + \frac{1}{4}\bar{v}_{13,46'}\frac{1}{-\varepsilon_{246'}}\bar{v}_{26',56}. \tag{D13}$$

The first term is equal to expression (D1). The second term is disconnected and, thus, is an inproper term for a vertex. The third term can be graphically represented as shown in Fig. 15. We see that the term of Fig. 15 is obtained from Fig. 12 in permuting indices 4 and 6. It is thus equivalent to the first term in Eq. (D13). This game can be repeated in the same way for the first and third terms in Eq. (D5). The conclusion is always the same: There are twice as many terms as equivalent terms from the on-shell version of Eq. (11), and in addition, each time there appears a disconnected term that should not be present in a vertex. However, this latter problem is not a real one. The order parameter is fully correlated, and no disconnected pieces can appear. The term that is disconnected in Eq. (D12) will certainly become connected in higher orders.

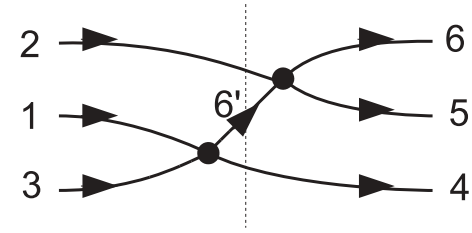

FIG. 15. Graphical expression of the third term on the right-hand side of Eq. (D13).

Therefore, such disconnected terms only serve to renormalize the vertices of the connected terms. In the end, all bare vertices in the connected diagrams should be replaced by two-body T matrices, and no disconnected terms would appear anymore. We will not dwell further on this point and simply discard the disconnected terms.

The conclusion, therefore, is that from Eq. (D3) we get twice as many terms for the vertex $\Gamma^{(3)}$ as is given in Eq. (11). Otherwise, the terms are equivalent under the condition that in Eq. (11), we take for these terms the on-shell prescription. The correct procedure, therefore, is to divide the vertices $V_{123;1'2'3'}$ in Eq. (D4) by a factor of 2. In the quartet case, we have to divide the vertex in Eq. (D10) by a factor of 8.

In our numerical application (quartet case), instead of calculating all 36 terms, where several ones give equal contributions resulting from squaring the vertex (D10) and where some are more difficult to calculate than others, we take a very pragmatic point of view and keep only the first term on the right-hand side of Eq. (D10) and simulate all the others by a factor of λ' as in Eq. (18). In doing so, we suppose that all terms have more or less the same analytic structure. This is certainly the case, because all the terms are dominated by the behavior of the 3h level density, whose typical structure is displayed in Sec. V. It also is fortunate that the final result does not depend on λ', as we now demonstrate on the example of pairing.

APPENDIX E: INDEPENDENCE OF THE PARAMETER λ' IN EQ. (18)

All arguments and derivations for the three-body vertices can directly be generalized to the four-body case. In view of the fact that our favorite expression (8) is too complex for a direct numerical realization, we take a very pragmatic point of view for a pilot application. We have seen that some terms appear in all the three forms we discussed for the vertices. We take one of those terms for numerical calculations with a parameter λ' in front of the vertex, which should demonstrate the influences of factors and of topologically different graphs. However, we stress again that we do not think that topologically different vertices will finally give rise to a different analytic structure of the mass operator. Essentially, these additional terms will again only renormalize the vertices. The form that we then retain is just the first one on the right-hade side of Eq. (D10), because it is the one where the single-particle motion directly

couples via an interaction to the quartet amplitude, that is,

$$\tilde{\Delta}_{1234} = \lambda' \tfrac{1}{2} \bar{v}_{12,1'2'} \delta_{33'} \delta_{44'} \langle c_{1'} c_{2'} c_{3'} c_{4'} \rangle. \tag{E1}$$

With the separable form of the two body interaction [22], we then obtain expression (21). As mentioned already, we approximately absorb factors and all the other terms in renormalizing the vertex by a constant factor λ'. This is a quite valid procedure, because the analytic structures of all the other terms are very similar. Fortunately, our results do not depend on the strength of the renormalization factor λ' of the vertex. This statement may be surprising but can be explained by the standard BCS example as follows.

Schematically, we write the expression for a single-particle GF in the BCS approximation of Eqs. (1) and (2) as follows (with self-evident notation):

$$G^{\mathrm{BCS}} = \frac{1}{\omega - \varepsilon - [(v\langle cc\rangle\langle c^\dagger c^\dagger\rangle v)/(\omega + \varepsilon)]}. \tag{E2}$$

Now in this equation, let us change the vertex v to $v' = \lambda' v$. Let us apply to all quantities containing this new vertex a "prime." Then the BCS single-particle GF is given by

$$G'^{\mathrm{BCS}} = \frac{1 - \rho'}{\omega - E'} + \frac{\rho'}{\omega + E'}, \tag{E3}$$

with $E'^2 = \varepsilon^2 + D'^2$, $D' = v'\langle cc\rangle$, and $\rho' = (1 - \varepsilon/E')/2$. The equation for the order parameter then reads

$$\langle cc\rangle = -\frac{1 - 2\rho'}{2\varepsilon} v \langle cc\rangle, \tag{E4}$$

where we should notice that the v in that equation is still the original one, as in our four-body order parameter equation of Eqs. (C2) and (C5).

From this, we obtain the gap equation for Δ':

$$\Delta' = -\sum v \frac{\Delta'}{2E'}. \tag{E5}$$

By multiplying this equation with λ', we see that $E' = E$, and therefore nothing is changed in the BCS single-particle mass operator when multiplying the vertex by an arbitrary factor. When translated to our quartet problem, this implies that the question of multiplicity of diagrams discussed here is of no consequence for our numerical results. Of course, the addition of topologically different contributions to the vertex $\Gamma^{(4)}$ can change things slightly, but again one can imagine that, to a good approximation, it only renormalizes the vertex corresponding to the process, which we treat explicitly. Therefore, our approximate treatment of the single-particle mass operator with quartet condensate should be quite safe. With our separable ansatz for the two-body interaction, we then arrive to expression (21) of the mass operator.

APPENDIX F: PREPARATION OF MASS OPERATOR FOR NUMERICAL APPLICATION

In this section, we describe the final expression for numerical calculation of the mass operator of Eq. (21).

We again give the approximated mass operator

$$\begin{aligned}
M^{\mathrm{quartet}}(k_1,\omega) = {} & \int \frac{d^3k_2}{(2\pi)^3}\frac{d^3k_3}{(2\pi)^3}\frac{d^3k_4}{(2\pi)^3}\frac{d^3k_{1'}}{(2\pi)^3}\frac{d^3k_{2'}}{(2\pi)^3}\frac{d^3k_{1''}}{(2\pi)^3}\frac{d^3k_{2''}}{(2\pi)^3} e^{-2(\vec{k}_1-\vec{k}_2)^2/(4b^2)} e^{-(\vec{k}_{1'}-\vec{k}_{2'})^2/(4b^2)} e^{-(\vec{k}_{1''}-\vec{k}_{2'''})^2/(4b^2)} (2\pi)^3 \\
& \times \delta(\vec{k}_1 + \vec{k}_2 - \vec{k}_{1'} - \vec{k}_{2'}) \varphi(|\vec{k}_{1'}|)\varphi(|\vec{k}_{2'}|)\varphi(|\vec{k}_3|)\varphi(|\vec{k}_4|)(2\pi)^3\delta(\vec{k}_{1'} + \vec{k}_{2'} + \vec{k}_3 + \vec{k}_4)\varphi(|\vec{k}_{1''}|)\varphi(|\vec{k}_{2''}|)\varphi(|\vec{k}_3|) \\
& \times \varphi(|\vec{k}_4|)(2\pi)^3\delta(\vec{k}_{1''} + \vec{k}_{2''} + \vec{k}_3 + \vec{k}_4) \frac{\bar{f}(k_2)\bar{f}(k_3)\bar{f}(k_4) + f(k_2)f(k_3)f(k_4)}{\omega + \varepsilon_{\vec{k}_2} + \varepsilon_{\vec{k}_3} + \varepsilon_{\vec{k}_4}} \\
= {} & \int \frac{d^3k_2}{(2\pi)^3}\frac{d^3K}{(2\pi)^3}\frac{d^3k}{(2\pi)^3}\frac{d^3K'}{(2\pi)^3}\frac{d^3k'}{(2\pi)^3}\frac{d^3K''}{(2\pi)^3}\frac{d^3k''}{(2\pi)^3} e^{-2(\vec{k}_1-\vec{k}_2)^2/(4b^2)} e^{-k'^2/b^2} e^{-k''^2/b^2} (2\pi)^3\delta(\vec{k}_1 + \vec{k}_2 - \vec{K}') \\
& \times \varphi\left(\left|\frac{\vec{K}'}{2} + \vec{k}'\right|\right)\varphi\left(\left|\frac{\vec{K}'}{2} - \vec{k}'\right|\right)\varphi\left(\left|\frac{\vec{K}}{2} + \vec{k}\right|\right)\varphi\left(\left|\frac{\vec{K}}{2} - \vec{k}\right|\right)(2\pi)^3\delta(\vec{K}' + \vec{K}) \\
& \times \varphi\left(\left|\frac{\vec{K}''}{2} + \vec{k}''\right|\right)\varphi\left(\left|\frac{\vec{K}''}{2} - \vec{k}''\right|\right)\varphi\left(\left|\frac{\vec{K}}{2} + \vec{k}\right|\right)\varphi\left(\left|\frac{\vec{K}}{2} - \vec{k}\right|\right)(2\pi)^3\delta(\vec{K}'' + \vec{K}) \\
& \times \frac{\bar{f}(k_2)\bar{f}[|(\vec{K}/2) + \vec{k}|]\bar{f}[|(\vec{K}/2) - \vec{k}|] + f(k_2)f[|(\vec{K}/2) + \vec{k}|]f[|(\vec{K}/2) - \vec{k}|]}{\omega + \varepsilon_{\vec{k}_2} + \varepsilon_{(\vec{K}/2)+\vec{k}} + \varepsilon_{(\vec{K}/2)-\vec{k}}} \\
= {} & \int \frac{d^3K}{(2\pi)^3}\frac{d^3k}{(2\pi)^3} e^{-2[\vec{k}_1 + (\vec{K}/2)]^2/b^2} \left[\varphi\left(\left|\frac{\vec{K}}{2} + \vec{k}\right|\right)\varphi\left(\left|\frac{\vec{K}}{2} - \vec{k}\right|\right)\right]^2 \\
& \times \frac{\bar{f}(|\vec{k}_1 + \vec{K}|)\bar{f}[|(\vec{K}/2) + \vec{k}|]\bar{f}[|(\vec{K}/2) - \vec{k}|] + f(|\vec{k}_1 + \vec{K}|)f[|(\vec{K}/2) + \vec{k}|]f[|(\vec{K}/2) - \vec{k}|]}{\omega + (k_1^2/2m) + [(\vec{k}_1 \cdot \vec{K})/m] + (3K^2/4m) + (k^2/m) - 3\mu} \\
& \times \left[\int \frac{d^3k'}{(2\pi)^3} e^{-k'^2/b^2} \varphi\left(\left|-\frac{\vec{K}}{2} + \vec{k}'\right|\right)\varphi\left(\left|-\frac{\vec{K}}{2} - \vec{k}'\right|\right)\right]^2.
\end{aligned} \tag{F1}$$

The imaginary part of the mass operator $-\mathrm{Im}M^{\mathrm{quartet}}(k_1, \omega + i\eta)$ is

$$
\begin{aligned}
&-\mathrm{Im}M^{\mathrm{quartet}}(k_1, \omega + i\eta) \\
&= \pi \int \frac{d^3K}{(2\pi)^3} \frac{d^3k}{(2\pi)^3} e^{-2[\vec{k}_1 + (\vec{K}/2)]^2/b^2} \\
&\quad \times \left[\varphi\left(\left| \frac{\vec{K}}{2} + \vec{k} \right| \right) \varphi\left(\left| \frac{\vec{K}}{2} - \vec{k} \right| \right) \right]^2 \\
&\quad \times \left[\bar{f}(|\vec{k}_1 + \vec{K}|) \bar{f}\left(\left| \frac{\vec{K}}{2} + \vec{k} \right| \right) \bar{f}\left(\left| \frac{\vec{K}}{2} - \vec{k} \right| \right) \right. \\
&\quad \left. + f(|\vec{k}_1 + \vec{K}|) f\left(\left| \frac{\vec{K}}{2} + \vec{k} \right| \right) f\left(\left| \frac{\vec{K}}{2} - \vec{k} \right| \right) \right] \\
&\quad \times \delta\left(\omega + \frac{k_1^2}{2m} + \frac{\vec{k}_1 \cdot \vec{K}}{m} + \frac{3K^2}{4m} + \frac{k^2}{m} - 3\mu \right) \\
&\quad \times \left[\int \frac{d^3k'}{(2\pi)^3} e^{-k'^2/b^2} \varphi\left(\left| -\frac{\vec{K}}{2} + \vec{k}' \right| \right) \right. \\
&\quad \left. \times \varphi\left(\left| -\frac{\vec{K}}{2} - \vec{k}' \right| \right) \right]^2 \qquad \text{(F2)}
\end{aligned}
$$

1. The $\vec{k}_1 = 0$ case

The imaginary part of the mass operator for $\vec{k}_1 = 0$ is given by

$$
\begin{aligned}
&-\mathrm{Im}M^{\mathrm{quartet}}(k_1 = 0, \omega + i\eta) \\
&= \pi \int \frac{d^3K}{(2\pi)^3} \frac{d^3k}{(2\pi)^3} e^{-K^2/(4b^2)} \\
&\quad \times \left[\varphi\left(\left| \frac{\vec{K}}{2} + \vec{k} \right| \right) \varphi\left(\left| \frac{\vec{K}}{2} - \vec{k} \right| \right) \right]^2 \\
&\quad \times \left[\bar{f}(K) \bar{f}\left(\left| \frac{\vec{K}}{2} + \vec{k} \right| \right) \bar{f}\left(\left| \frac{\vec{K}}{2} - \vec{k} \right| \right) \right. \\
&\quad \left. + f(K) f\left(\left| \frac{\vec{K}}{2} + \vec{k} \right| \right) f\left(\left| \frac{\vec{K}}{2} - \vec{k} \right| \right) \right] \\
&\quad \times \delta\left(\omega + \frac{3K^2}{4m} + \frac{k^2}{m} - 3\mu \right) \left[\int \frac{d^3k'}{(2\pi)^3} e^{-k'^2/b^2} \right. \\
&\quad \left. \times \varphi\left(\left| -\frac{\vec{K}}{2} + \vec{k}' \right| \right) \varphi\left(\left| -\frac{\vec{K}}{2} - \vec{k}' \right| \right) \right]^2 \\
&= \pi \frac{2}{(2\pi)^4} \int_0^\infty dK K^2 \int_0^\infty dk k^2 \int_{-1}^1 dt e^{-K^2/(4b^2)} \\
&\quad \times \left[\varphi\left(\left| \frac{\vec{K}}{2} + \vec{k} \right| \right) \varphi\left(\left| \frac{\vec{K}}{2} - \vec{k} \right| \right) \right]^2 \\
&\quad \times \left[\bar{f}(K) \bar{f}\left(\left| \frac{\vec{K}}{2} + \vec{k} \right| \right) \bar{f}\left(\left| \frac{\vec{K}}{2} - \vec{k} \right| \right) \right. \\
&\quad \left. + f(K) f\left(\left| \frac{\vec{K}}{2} + \vec{k} \right| \right) f\left(\left| \frac{\vec{K}}{2} - \vec{k} \right| \right) \right] \\
&\quad \times \frac{m}{2k} \delta(k - \sqrt{3m\mu - m\omega - 3K^2/4}) \\
&\quad \times \left[\frac{1}{(2\pi)^2} \int_0^\infty dk' k'^2 \int_{-1}^1 dt' e^{-k'^2/b^2} \right. \\
&\quad \left. \times \varphi\left(\left| -\frac{\vec{K}}{2} + \vec{k}' \right| \right) \varphi\left(\left| -\frac{\vec{K}}{2} - \vec{k}' \right| \right) \right]^2 \\
&= \frac{2\pi m}{2(2\pi)^4} \int_0^{P_{max0}} dK K^2 p \int_{-1}^1 dt e^{-K^2/(4b^2)} \\
&\quad \times \left[\varphi\left(\left| \frac{\vec{K}}{2} + \vec{p} \right| \right) \varphi\left(|\frac{\vec{K}}{2} - \vec{p}| \right) \right]^2 \\
&\quad \times \left[\bar{f}(K) \bar{f}\left(\left| \frac{\vec{K}}{2} + \vec{p} \right| \right) \bar{f}\left(|\frac{\vec{K}}{2} - \vec{p}| \right) \right. \\
&\quad \left. + f(K) f\left(\left| \frac{\vec{K}}{2} + \vec{p} \right| \right) f\left(|\frac{\vec{K}}{2} - \vec{p}| \right) \right] \\
&\quad \times \left[\frac{1}{(2\pi)^2} \int_0^\infty dk' k'^2 \int_{-1}^1 dt' e^{-k'^2/b^2} \right. \\
&\quad \left. \times \varphi\left(\left| -\frac{\vec{K}}{2} + \vec{k}' \right| \right) \varphi\left(\left| -\frac{\vec{K}}{2} - \vec{k}' \right| \right) \right]^2, \qquad \text{(F3)}
\end{aligned}
$$

Here, in the last equation,

$$p = \sqrt{3m\mu - m\omega - \frac{3K^2}{4}}, \qquad \text{(F4)}$$

$$P_{\mathrm{max0}} = \sqrt{\frac{4}{3}(3m\mu - m\omega)}, \qquad \text{(F5)}$$

$$t = (\vec{p} \cdot \vec{K})/(pK), \qquad \text{(F6)}$$

$$t' = (\vec{k}' \cdot \vec{K})/(k'K). \qquad \text{(F7)}$$

2. The $\vec{k}_1 \neq 0$ case

On the other hand, $-\mathrm{Im}M^{\mathrm{quartet}}$ for $\vec{k}_1 \neq 0$ is represented by

$$
\begin{aligned}
&-\mathrm{Im}M^{\mathrm{quartet}}(k_1, \omega + i\eta) \\
&= \frac{\pi}{(2\pi)^4} \int_0^\infty dK K^2 \int_{-1}^1 dt_1 \int_0^\infty dk k^2 \int_{-1}^1 dt \\
&\quad \times e^{-2(k_1^2 + K^2/4 + k_1 K t_1)/b^2} \left[\varphi\left(\left| \frac{\vec{K}}{2} + \vec{k} \right| \right) \varphi\left(\left| \frac{\vec{K}}{2} - \vec{k} \right| \right) \right]^2 \\
&\quad \times \left[\bar{f}(|\vec{k}_1 + \vec{K}|) \bar{f}\left(\left| \frac{\vec{K}}{2} + \vec{k} \right| \right) \bar{f}\left(\left| \frac{\vec{K}}{2} - \vec{k} \right| \right) \right. \\
&\quad \left. + f(|\vec{k}_1 + \vec{K}|) f\left(\left| \frac{\vec{K}}{2} + \vec{k} \right| \right) f\left(\left| \frac{\vec{K}}{2} - \vec{k} \right| \right) \right] \\
&\quad \times \delta\left(\omega + \frac{k_1^2}{2m} + \frac{k_1 K t_1}{m} + \frac{3K^2}{4m} + \frac{k^2}{m} - 3\mu \right)
\end{aligned}
$$

$$\times \left[\frac{1}{(2\pi)^2}\int dk' k'^2 \int_{-1}^{1} dt' e^{-k'^2/b^2} \times \varphi\left(\left|-\frac{\vec{K}}{2}+\vec{k}'\right|\right)\varphi\left(\left|-\frac{\vec{K}}{2}-\vec{k}'\right|\right)\right]^2$$

$$= \frac{\pi}{(2\pi)^4}\int_0^\infty dK K^2 \int_{-1}^{1} dt_1 \int_0^\infty dk k^2 \int_{-1}^{1} dt \times e^{-2(k_1^2+K^2/4+k_1 K t_1)/b^2}\left[\varphi\left(\left|\frac{\vec{K}}{2}+\vec{k}\right|\right)\varphi\left(\left|\frac{\vec{K}}{2}-\vec{k}\right|\right)\right]^2 \times \left[\bar{f}(|\vec{k}_1+\vec{K}|)\bar{f}\left(\left|\frac{\vec{K}}{2}+\vec{k}\right|\right)\bar{f}\left(\left|\frac{\vec{K}}{2}-\vec{k}\right|\right) + f(|\vec{k}_1+\vec{K}|)f\left(\left|\frac{\vec{K}}{2}+\vec{k}\right|\right)f\left(\left|\frac{\vec{K}}{2}-\vec{k}\right|\right)\right] \times \frac{m}{k_1 K}\delta\left(t_1 - \frac{3m\mu - m\omega - (k_1^2/2) - (3K^2/4) - k^2}{k_1 K}\right) \times \left[\frac{1}{(2\pi)^2}\int dk' k'^2 \int_{-1}^{1} dt' e^{-k'^2/b^2} \times \varphi\left(\left|-\frac{\vec{K}}{2}+\vec{k}'\right|\right)\varphi\left(\left|-\frac{\vec{K}}{2}-\vec{k}'\right|\right)\right]^2. \quad \text{(F8)}$$

Here, the following condition has to be satisfied:

$$-1 < \frac{3m\mu - m\omega - (k_1^2/2) - (3K^2/4) - k^2}{k_1 K} < 1. \quad \text{(F9)}$$

Therefore,

$$k^2 > 3m\mu - m\omega - \frac{k_1^2}{2} - \frac{3K^2}{4} - k_1 K > 0 \quad \text{(F10)}$$

and

$$0 < k^2 < 3m\mu - m\omega - \frac{k_1^2}{2} - \frac{3K^2}{4} + k_1 K. \quad \text{(F11)}$$

From this equation, we obtain the limits of integration with respect to k:

$$p_{\min}(K) = \sqrt{\max(3m\mu - m\omega - \frac{k_1^2}{2} - \frac{3K^2}{4} - k_1 K, 0)} < k < \sqrt{3m\mu - m\omega - \frac{k_1^2}{2} - \frac{3K^2}{4} + k_1 K} = p_{\max}(K). \quad \text{(F12)}$$

Besides, from Eq. (F11),

$$3m\mu - m\omega - \frac{k_1^2}{2} - \frac{3K^2}{4} + k_1 K > 0 \quad \text{(F13)}$$

has to be satisfied. Therefore,

$$P_{\min} = \max\left[\frac{2}{3}\left(k_1 - \sqrt{9m\mu - 3m\omega - \frac{k_1^2}{2}}\right), 0\right] < K < \frac{2}{3}\left(k_1 + \sqrt{9m\mu - 3m\omega - \frac{k_1^2}{2}}\right) = P_{\max}. \quad \text{(F14)}$$

3. Summary of integrals in $\mathrm{Im}M^{\mathrm{quartet}}$

With the Appendices F1 and F2, we can express $-\mathrm{Im}M^{\mathrm{quartet}}(k_1, \omega + i\eta)$ as follows:

If $9m\mu - 3m\omega - \frac{k_1^2}{2} < 0$,

$$-\mathrm{Im}M^{\mathrm{quartet}}(k_1, \omega + i\eta) = 0. \quad \text{(F15)}$$

Else:

If $k_1 = 0$,

$$-\mathrm{Im}M^{\mathrm{quartet}}(k_1, \omega + i\eta) = \frac{2\pi m}{2(2\pi)^4}\int_0^{P_{\max 0}} dK K^2 p e^{-K^2/(4b^2)} \times \int_{-1}^{1} dt \left[\varphi\left(\left|\frac{\vec{K}}{2}+\vec{p}\right|\right)\varphi\left(\left|\frac{\vec{K}}{2}-\vec{p}\right|\right)\right]^2 \times \left[\bar{f}(K)\bar{f}\left(\left|\frac{\vec{K}}{2}+\vec{p}\right|\right)\bar{f}\left(\left|\frac{\vec{K}}{2}-\vec{p}\right|\right) + f(K)f\left(\left|\frac{\vec{K}}{2}+\vec{p}\right|\right)f\left(\left|\frac{\vec{K}}{2}-\vec{p}\right|\right)\right] \times \left[\frac{1}{(2\pi)^2}\int_0^\infty dk' k'^2 e^{-k'^2/b^2}\int_{-1}^{1} dt' \times \varphi\left(\left|-\frac{\vec{K}}{2}+\vec{k}'\right|\right)\varphi\left(\left|-\frac{\vec{K}}{2}-\vec{k}'\right|\right)\right]^2,$$

$$p = \sqrt{3m\mu - m\omega - \frac{3K^2}{4}},$$

$$P_{\max 0} = \sqrt{\frac{4}{3}(3m\mu - m\omega)},$$

$$t = (\vec{k}\cdot\vec{K})/(kK), \quad t' = (\vec{k}'\cdot\vec{K})/(k'K), \quad \text{(F16)}$$

while if $k_1 \neq 0$,

$$-\mathrm{Im}M^{\mathrm{quartet}}(k_1, \omega + i\eta) = \frac{\pi m}{(2\pi)^4 k_1}\int_{P_{\min}}^{P_{\max}} dK K \int_{p_{\min}}^{p_{\max}} dk k^2 \times e^{-2(3m\mu - m\omega + k_1^2/2 - K^2/2 - k^2)/b^2} \times \int_{-1}^{1} dt \left[\varphi\left(\left|\frac{\vec{K}}{2}+\vec{k}\right|\right)\varphi\left(\left|\frac{\vec{K}}{2}-\vec{k}\right|\right)\right]^2 \times \left[\bar{f}\left(\sqrt{6m\mu - 2m\omega - \frac{K^2}{2} - 2k^2}\right)\bar{f}\left(\left|\frac{\vec{K}}{2}+\vec{k}\right|\right) \times \bar{f}\left(\left|\frac{\vec{K}}{2}-\vec{k}\right|\right) + f\left(\sqrt{6m\mu - 2m\omega - \frac{K^2}{2} - 2k^2}\right) \times f\left(\left|\frac{\vec{K}}{2}+\vec{k}\right|\right)f\left(\left|\frac{\vec{K}}{2}-\vec{k}\right|\right)\right] \times \left[\frac{1}{(2\pi)^2}\int_0^\infty dk' k'^2 e^{-k'^2/b^2}\int_{-1}^{1} dt'\right.$$

$$\times \varphi\left(\left|-\frac{\vec{K}}{2}+\vec{k}'\right|\right)\varphi\left(\left|-\frac{\vec{K}}{2}-\vec{k}'\right|\right)\Bigg]^2,$$

$$p_{\min}(K)=\sqrt{\max\left[3m\mu-m\omega-\frac{k_1^2}{2}-\frac{3K^2}{4}-k_1K,0\right]},$$

$$p_{\max}(K)=\sqrt{3m\mu-m\omega-\frac{k_1^2}{2}-\frac{3K^2}{4}+k_1K},$$

$$P_{\min}=\max\left[\frac{2}{3}\left(k_1-\sqrt{9m\mu-3m\omega-\frac{k_1^2}{2}}\right),0\right],$$

$$P_{\max}=\frac{2}{3}\left(k_1+\sqrt{9m\mu-3m\omega-\frac{k_1^2}{2}}\right),$$

$$t=(\vec{k}\cdot\vec{K})/(kK),\quad t'=(\vec{k}'\cdot\vec{K})/(k'K). \tag{F17}$$

$\mathrm{Re}M^{\mathrm{quartet}}$ is calculated by Eq. (22).

[1] A. Tohsaki, H. Horiuchi, P. Schuck, and G. Röpke, Phys. Rev. Lett. **87**, 192501 (2001); Y. Funaki, T. Yamada, H. I. Horiuchi, G. Röpke, P. Schuck, and A. Tohsaki, *ibid.* **101**, 082502 (2008).

[2] S. Typel, G. Röpke, T. Klähn, D. Blaschke, and H. H. Wolter, Phys. Rev. C **81**, 015803 (2010).

[3] A. N. Wenz, T. Lompe, T. B. Ottenstein, F. Serwane, G. Zürn, and S. Jochim, Phys. Rev. A **80**, 040702(R) (2009).

[4] J. R. Williams, E. L. Hazlett, J. H. Huckans, R. W. Stites, Y. Zhang, and K. M. O'Hara, Phys. Rev. Lett. **103**, 130404 (2009).

[5] Á. Rapp, G. Zaránd, C. Honerkamp, and W. Hofstetter, Phys. Rev. Lett. **98**, 160405 (2007).

[6] X. W. Guan, M. T. Batchelor, C. Lee, and H.-Q. Zhou, Phys. Rev. Lett. **100**, 200401 (2008).

[7] A. Kantian, M. Dalmonte, S. Diehl, W. Hofstetter, P. Zoller, and A. J. Daley, Phys. Rev. Lett. **103**, 240401 (2009).

[8] S. Floerchinger, R. Schmidt, and C. Wetterich, Phys. Rev. A **79**, 053633 (2009).

[9] B. Errea, J. Dukelsky, and G. Ortiz, Phys. Rev. A **79**, 051603(R) (2009).

[10] T. N. De Silva, Phys. Rev. A **80**, 013620 (2009).

[11] R. A. Molina, J. Dukelsky, and P. Schmitteckert, Phys. Rev. A **80**, 013616 (2009).

[12] P. Azaria, S. Capponi, and P. Lecheminant, Phys. Rev. A **80**, 041604(R) (2009).

[13] S.-Y. Miyatake, K. Inaba, and S.-I. Suga, Phys. Rev. A **81**, 021603(R) (2010).

[14] H. Kamei and K. Miyake, J. Phys. Soc. Jpn. **74**, 1911 (2005).

[15] A. S. Stepanenko and J. M. F. Gunn, arXiv:cond-mat/9901317.

[16] P. Schlottmann, J. Phys. Condens. Matter **6**, 1359 (1994).

[17] C. Wu, Phys. Rev. Lett. **95**, 266404 (2005).

[18] G. Roux, S. Capponi, P. Lecheminant, and P. Azaria, Eur. Phys. J. B **68**, 293 (2009).

[19] M. Hasuo and N. Nagasawa, in *Bose-Einstein Condensation*, edited by A. Griffin, D. W. Snoke, and S. Stringari (Cambridge University Press, Cambridge, 1995), p. 487.

[20] S. A. Moskalenko and D. W. Snoke, *Bose-Einstein Condensation of Excitons and Biexcitons* (Cambridge University Press, Cambridge, 2000).

[21] T. Sogo, R. Lazauskas, G. Röpke, and P. Schuck, Phys. Rev. C **79**, 051301(R) (2009).

[22] G. Röpke, A. Schnell, P. Schuck, and P. Nozières, Phys. Rev. Lett. **80**, 3177 (1998).

[23] D. J. Thouless, Ann. Phys. **10**, 553 (1960).

[24] P. Ring and P. Schuck, *The Nuclear Many-Body Problem* (Springer-Verlag, New York, 1980).

[25] A. A. Abrikosov, L. P. Gorkov, and I. E. Dzyaloshinski, *Methods of Quantum Field Theory in Statistical Physics* (Dover, New York, 1975).

[26] A. L. Fetter and J. D. Walecka, *Quantum Theory of Many-Particle Systems* (Dover, New York, 2003).

[27] J. G. Hirsch, A. Mariano, J. Dukelsky, and P. Schuck, Ann. Phys. **296**, 187 (2002).

[28] S. Adachi and P. Schuck, Nucl. Phys. A **496**, 485 (1989).

[29] A. H. Blin, R. W. Hasse, B. Hiller, P. Schuck, and C. Yannouleas, Nucl. Phys. A **456**, 109 (1986).

[30] J. Dukelsky, G. Röpke, and P. Schuck, Nucl. Phys. A **628**, 17 (1998).

[31] G. D. Mahan, *Many-Particle Physics* (Plenum, New York, 1990).